AD-A265 727

DISTRIBUTED COMBUSTION
IN
SOLID PROPELLANTS
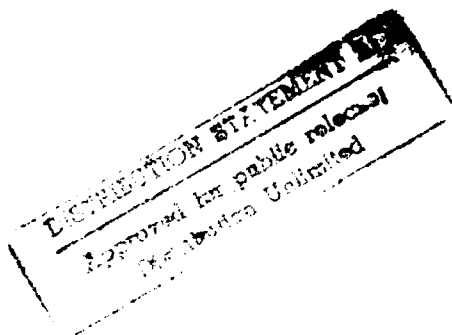
by

M.W. BECKSTEAD and K. P. BROOKS
BRIGHAM YOUNG UNIVERSITY
PROVO, UTAH

May 1993

JUN 14 1993

Prepared for

93-13289

REPORT DOCUMENTATION PAGE

1. AGENCY USE ONLY (Leave blank)	2. REPORT DATE May 1993	3. REPORT TYPE AND DATES COVERED Final Report Feb. 1, 1991 - Feb. 1, 1993

4. TITLE AND SUBTITLE

Distributed Combustion in Solid Propellants

6. AUTHOR(S)

M.W. Beckstead and K.P. Brooks

5. FUNDING NUMBERS

PE - 61102F
PR - 2308
SA - AS
G - AFOSR-91
-0152

7. PERFORMING ORGANIZATION NAME(S) AND ADDRESS(ES)

Brigham Young University
Dept. of Chemical Engineering
Provo, UT 84602

8. PERFORMING ORGANIZATION REPORT NUMBER

9. SPONSORING/MONITORING AGENCY NAME(S) AND ADDRESS(ES)

AFOSR/NA
110 Duncan Avenue Suite B115
Bolling AFB DC 20332-0001

10. SPONSORING/MONITORING AGENCY REPORT NUMBER

11. SUPPLEMENTARY NOTES

12a. DISTRIBUTION/AVAILABILITY STATEMENT

Approved for public release; distribution is unlimited

12b. DISTRIBUTION CODE

13. ABSTRACT (Maximum 200 words)

This report summarizes work on a research program to quantify the effect of distributed combustion of metal particles in a Rijke burner. Under a previous contract experimental data were obtained with the Rijke burner, and a mathematical model of the burner was developed. To improve the model, the McIntosh flame model, based on large activation energy asymptotics, has been coupled to the acoustic model. Results have been compared to experimental data showing that the McIntosh transfer function is an improvement over previous models.

Law's model of aluminum combustion has been modified to include the effects of multiple oxidizers and their products, oxide accumulation on the surface of the burning aluminum particle, and convection. There are no adjustable parameters in the improved aluminum combustion model, and both transport and thermodynamic properties are calculated internally. Results indicate that the modified model compares more favorably to experimental data than a simple liquid droplet model. The aluminum combustion model has also been coupled to the Rijke acoustic model. Calculations show a sensitivity to the size of the region of influence surrounding a particle and to the time lag between the particle response and the acoustic pressure. The results show reasonable agreement with available data for aluminum particles burning in the Rijke burner.

14. SUBJECT TERMS

Unstable Combustion, Distributed Combustion
Acoustic Instability

15. NUMBER OF PAGES
51

16. PRICE CODE

17. SECURITY CLASSIFICATION OF REPORT	18. SECURITY CLASSIFICATION OF THIS PAGE	19. SECURITY CLASSIFICATION OF ABSTRACT	20. LIMITATION OF ABSTRACT
Unclassified	Unclassified	Unclassified	UL

TABLE OF CONTENTS

A-1

LIST OF FIGURES

LIST OF TABLES

NOMENCLATURE

A	Area (m^2)
a	Radius of the oxide cap attached to an aluminum particle (m)
a_k	Sum of the mole fractions of the oxidizers in Eq. (3.1)
C	Concentration (mol/m^3)
C_p	Heat capacity (J/kg)
D	Diffusivity (m^2/s); Rijke burner diameter (m)
d	Particle diameter (m)
E_a	Activation Energy (cal/mol)
F	Ratio of total mass flux to mass flux aluminum
H	Rate of energy release (W); total flux of energy in aluminum combustion model (W/m^2); heat of reaction (J/mol)
h	Defined in Eq. (6.8)
J	Factor used to correct the lean species Lewis number
j	Mass flux due to diffusion ($kg/m^2/s$)
k	Arbitrary constant in Eq. (3.1)
Le	Lewis number
M	Mach number; Non-dimensional mass flux used in aluminum combustion model
m	Mass flux ($kg/m^2/s$)
m_c	Mass flux condensed metal oxide ($kg/m^2/s$)
m_v	Mass flux vaporized metal oxide ($kg/m^2/s$)
n	Arbitrary exponential to the diameter; order of the reaction
Nu	Nusselt number
p	Pressure (N/m^2)
Pr	Prandtl number
q	Heat flux (W/m^2)
Q_r	Heat production due to a reaction (W/m^3); Heat caused by radiation (W/m^2)
R	Universal gas constant; volume fraction condensed oxide
r	Radial distance (m); reaction rate ($kg/m^3/s$)
Re	Reynolds number
Sc	Schmidt number

T	Temperature (K)
t	Time (sec)
T_{01}	Ratio of unburnt gas temperature to burnt gas temperature in Eq. (2.3)
u_{u0}	Acoustic velocity upstream of the flame in Eq. (2.3) (m/s)
$u_{u\infty}$	Acoustic velocity downstream of the flame in Eq. (2.3) (m/s)
V	Transfer function for McIntosh flame model in Eq. (2.3)
v	Velocity (m/s); volume (m^3)
w	Transport property weighting factor
x	Axial distance in the Rijke burner; mole fraction
Y	Mass fraction of a gas species
Z	Impedance of the flame holder ($N\text{-}s/m^3$)

Greek Symbols

α	Acoustic growth rate (1/sec)
Δ_l	Mixture strength constant (mol/m^3)
ΔH_{rxn}	Heat of reaction (kcal/mol)
ΔH_{vap}	Heat of vaporization (kcal/mol)
Φ	Equivalence Ratio
ϕ	Any given transport property
γ	Ratio of specific heats
η	Fraction of vaporized oxide which moves toward the particle surface
λ	Thermal conductivity (W/m/K)
ν	Stoichiometric mass ratio of oxide or oxidizer to metal
θ	Fraction of metal oxide which vaporizes at the flame
θ_1	Non-dimensional activation energy
ρ	Density (kg/m^3)
τ	Characteristic time lag (sec)
ω	Complex frequency , $\omega_0 - i\alpha$ (sec^{-1})
ω_0	Angular frequency (sec^{-1})
ξ	Fraction of condensed products with move inward or outward
Ψ	Arbitrary complex constant

Subscripts

0	zeroth perturbation in activation energy asymptotics
1	first perturbation in activation energy asymptotics
A	region between particle surface and flame
a	adiabatic value
B	region between flame and infinity
b	burnt value
c	critical; or condensed oxide

f	flame
g	gas
i	gas species
inf	location of edge of boundary layer
l	lean
o	atomic oxygen available for reaction
p	particle
r	reaction; or rich
s	particle surface
v	vaporized oxide

Superscripts

^	acoustic property with time dependency removed; non dimensional
'	acoustic property including time dependency; dimensional parameter
-	mean property
•	high mass flux

1.0 INTRODUCTION AND MOTIVATION

1.1 Motivation for Study of Distributed Combustion

In 1974 and 1975 M.W. Beckstead and F.E.C. Culick (Culick, 1974,1975) began discussing the effects that aluminum particles could have on acoustics when those particles burn relatively far from the burning propellant surface. Test data in several devices, primarily the T-burner, showed results inconsistent with the then state-of-the-art theory for combustion instability. Data for non-metallized propellants appeared to be relatively consistent, but metallized propellants seemed to give inconsistent results. Culick wrote two memos outlining some the effects that burning particles could have on a system through interaction with an acoustic wave. In 1979 Beckstead, then at Brigham Young University, submitted a proposal to AFOSR with one task designated to study the concept of 'distributed combustion', the interaction of burning particle on an acoustic wave. This began a modest research effort on distributed combustion. As part of the program a propane fired Rijke burner was developed to aid in studying the phenomenon (e.g. Braithewaite, 1984, Beckstead, et al, 1984, and Beckstead, 1984).

In 1983 the Army was involved in developing an antiballistic missile defense system, SENTRY. During that year three full scale development motors were test fired. All three motors experienced an unacceptably high level of combustion instability, and the entire development program was subsequently canceled. Calculations for the motors using standard stability analysis techniques indicated that the motors should have been stable. The motors operated in a high pressure range with a very high burning rate metallized propellant. A workshop with many prominent experts on combustion instability was held at NWC, China Lake to try to determine the cause of the combustion instability (Stone, 1984). All of the available motor data, test data and calculations were reviewed. The conclusion of the panel was that distributed combustion was most likely the cause of the problem. The AFOSR research programs had a significant contribution to the results of this workshop.

The SENTRY experience added impetus to the research effort. The AFOSR research continued , but was now focused on distributed combustion. Experimental work with the Rijke burner continued and a modeling effort was added to increase the analytical understanding. In addition, a long range program was begun at NWC working on developing capability to analyze and test for distributed combustion. Since then a high pressure T-burner facility has been constructed and is now in use to test high burn rate metallized propellants up to the high pressure of interest (e.g. Blomshield, et. al., 1991).

In 1989 the Army reinitiated an effort to develop an antiballistic missile defense system, which is now referred to as THAAD, Theater High Altitude Area Defense. A primary concern in the development program was the question of combustion instability. T-burner testing was performed at NWC to characterize several candidate propellants. Also, a small contract was let between Thiokol and Brigham Young University to incorporate the BYU developed modeling concepts of distributed combustion into the SSP (Standard Stability Program), and then analyze proposed motor designs for potential combustion instability. The BYU program also developed

the capability for analyzing T-burner data allowing for distributed combustion effects (Blomshield, et. al., 1991, Beckstead and Brooks, 1990). In 1990 a candidate design was analyzed with the modified SSP program. Using the NWC T-burner data the calculations indicated that the new propellant in the new design would be stable. The enhanced stability over the SENTRY design was due primarily to an improved internal design of the motor grain geometry.

Manufacturing of the motor proceeded, and in April 1992 the first test firing of the newly developed motor was conducted. The motor did not exhibit combustion instability, and further development and flight testing of the motor is now proceeding.

This is an excellent example of how basic research can anticipate potential problems, and be applied to those problems when they surface.

1.2 Using the Rijke Burner to Study Distributed Combustion

Researchers at Brigham Young University have designed a gas fired Rijke Burner (Braithewaite, 1984; Finlinson, 1988; Barron, 1991) to understand the interaction between the metal particle combustion and combustion instability. The Rijke burner is a propane flame held in place within an open or closed-ended steel tube. Propane gas was chosen because of the high flame temperature needed to ignite aluminum particles and its convenience. Organ-pipe type acoustic standing waves develop within the tube due to the interaction of the flame and the acoustics.

Metal particles can be entrained in the gases and will ignite after passing through the flame. Work with the Rijke burner has focused on measuring the acoustic growth rate in the burner, varying the geometry of the burner, mixture fraction of gases. and the metal particle characteristics in an effort to understand distributed combustion.

The use of a Rijke burner greatly simplifies the acoustic combustion instability phenomena found in rocket motors. Rather than the complex mode shapes found within a rocket motor, the Rijke burner has only axial harmonics. Unlike a rocket motor, which as it burns changes its physical dimensions, the Rijke burner dimensions remain constant. The Rijke burner can be tested over an extended period of time, whereas tests done with propellant cannot. In addition, many of the acoustic driving and damping effects are eliminated in the Rijke burner, thus reducing the number of factors to be understood.

These simplifications result in some limitations in the comparison between the Rijke burner and actual rocket motors. Since no propellant is used in the burne , the burn characteristics are different.

1.3 Theoretical Study of Distributed Combustion

In conjunction with the experimental work at Brigham Young University, a mathematical model of the Rijke burner has been developed by Raun (1985). This model predicts the frequencies and acoustic growth rates of the combustion driven oscillations in the Rijke burner both with and without particle combustion. Unlike other Rijke models, the Raun model appears to be more physically realistic and describes the acoustic aspects of the Rijke burner quite well. However, quantitative agreement between the model and experimental work has been difficult to attain.

A primary purpose of this current work is to improve the Raun's Rijke model. In addition, this study is an effort to improve the fundamental understanding of the physics of the Rijke Burner, aluminum combustion, and the interaction between the

aluminum and acoustic wave. The first phase of the study is to model the acoustic growth due to the propane flame better. The flame-acoustic interaction is the primary acoustic driving force in a Rijke burner. thus it must be understood before the secondary effects of aluminum combustion can be properly quantified. The second phase is an improved understanding of the aluminum combustion characteristics. as well as their influence on the acoustics of the Rijke burner.

2.0 RIJKE MODELING BACKGROUND

The Rijke phenomena is the production of sound in an enclosed chamber due to thermal/acoustic interactions. The tubes used to study the Rijke phenomena can be divided into two basic categories: those with flames. called Rijke burners and those without flames, known as Rijke tubes. A comprehensive review paper on Rijke related devices has recently been written in conjunction with this contract. The paper "A Review of Rijke Tubes. Rijke Burners and Related Devices" by Raun. Beckstead. Finlinson and Brooks has been accepted for publication in the journal. Progress in Combustion and Energy Science. Thus, this section will be very abbreviated.

2.1 Rayleigh Criterion

A criteria established by Rayleigh (1878) seems to be most successful in explaining the physical mechanism occurring in the Rijke tube. The Rayleigh criteria can be stated as follows: Oscillations will grow when heat is added at a point of greatest compression or removed at a point of greatest expansion. The criteria for acoustic driving to occur can be written mathematically as

$$\int_{cycle} Hp' \, dt > 0 \tag{2.1}$$

where H is the heat release and p' is the acoustic pressure. This theory. although qualitative in nature, has been used by nearly all researchers to explain and model the Rijke phenomena.

Modeling the Rijke burner is more complex than modeling the simpler Rijke tube. Not only is the oscillatory heat transfer important between the flame. flame holder and gas, but the motion and reaction rate of the flame itself interacts with the acoustics. There are three basic approaches used in modeling the flame in the Rijke burner: (1) the heat transfer approach. (2) the time lag approach. and (3) the large activation energy asymptotics approach. Because large activation energy asymptotics appears both comprehensive and tractable, it has been used in the current research.

2.2 Large Activation Energy Asymptotics Approach

Recently, a group of researchers have taken a very fundamental approach to understanding the interaction of the flame and acoustics using large activation energy

3

asymptotes. Because an exact solution to the conservation equations is not possible due to the nonlinear nature of the Arrhenius expression. activation energy asymptotics is used to achieve a solution.

The process involves an asymptotic expansion of temperature (T) and concentration (C) in terms of a non-dimensionalized activation energy of the form:

$$T = T_0 + \left(\frac{E_a}{R\,T_0}\right)^{-1} T_1 + \ldots \qquad C = C_0 + \left(\frac{E_a}{R\,T_0}\right)^{-1} C_1 + \ldots \qquad (2.2)$$

where R is the universal gas constant and T_0 is the cold gas temperature. The combustion zone is divided into (1) a preheat region between the flame holder and the flame, (2) the flame sheet. (3) and the equilibrium zone. The continuity equations of the preheat and equilibrium zones can easily be solved without the exponential term. In the region of the flame sheet, the temperature and concentration are replaced in the conservation equations by their expanded asymptotic series. These equations can then be solved analytically using the solutions of the preheat and equilibrium zone as boundary conditions. A closed form expression is obtained to describe the properties of the flame in the limit as activation energy to goes to infinity.

2.3 Steady State Model

Early work using these concepts was performed on the steady-state characteristics of flat flames anchored by a flame holder (Carrier. et. al., 1978; Clarke and McIntosh. 1980). From their solution. Clarke. et. al. was able to obtain a unique mass flux through the flame holder for any given value of the flame's burnt gas temperature. The location of the flame with respect to the flame holder was also obtained based on stoichiometry. diffusivity of the lean species. and heat loss.

2.4 Unsteady Flame Modeling

McIntosh and Clarke (1981) built on their previous work to determine the response of the pulsating flat flame to oscillatory inputs in composition and inlet mass flux. However. in addition to applying an asymptotic series in terms of activation energy to the flame zone. McIntosh also applies a small perturbation in the properties to allow for the oscillatory inputs. McIntosh (1986. 1987. 1990) further studied the interaction between an anchored flame and an acoustic wave. In these works. the acoustic velocity downstream of the flame ($\bar{u}_{u\infty}$) was obtained in terms of acoustic velocity upstream of the flame ($\bar{u}_{u0}$) :

$$\bar{u}_{u\infty} = -\frac{\bar{u}_{u0}V}{T_{01}} \qquad (2.3)$$

where T_{01} is the ratio of temperatures before and after the flame and V is a transfer function based on the complex frequency, Lewis number. and gas velocity upstream of the flame. (See Appendix A for details.)

McIntosh found that heat loss to the gauze. not tube length. is responsible for the resonant frequencies associated with unstable flame behavior. The amplification of the acoustic wave as it crosses the flame was found to be somewhat analogous to a

4

second order system. Comparing the model to experimental data. he found that maximum driving occurs when the flame holder is in the lower quadrant of the tube (the original Rijke observation). (See Figure 2.1.)
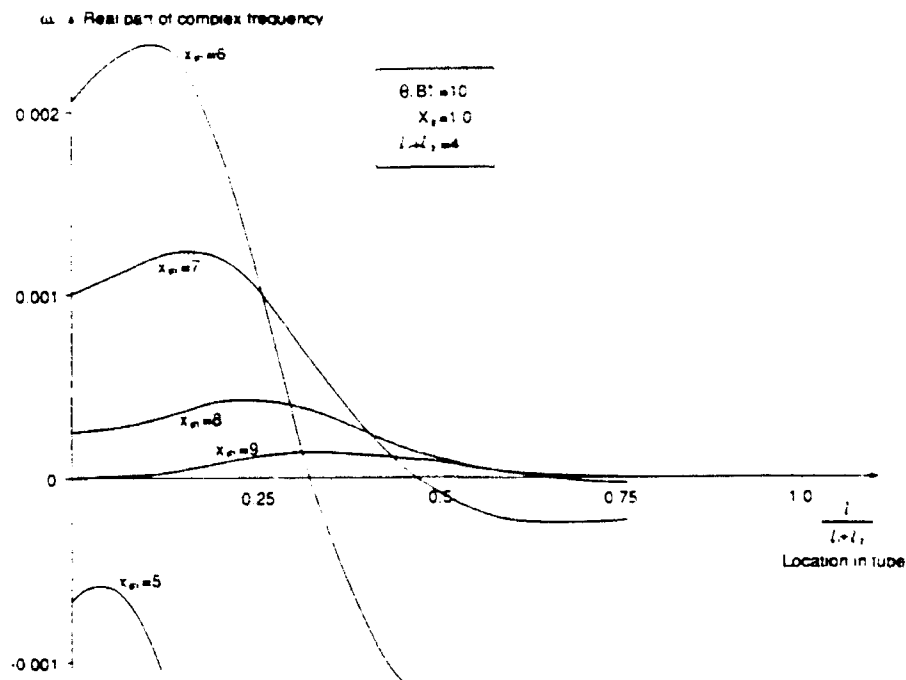
Figure 2.1 McIntosh flame model results. Acoustic growth rate as a function of location in the Rijke burner for several flame standoff distances (From McIntosh, 1990).

3.0 BACKGROUND OF ALUMINUM COMBUSTION

3.1 Aluminum in Rocket Motors

A typical composite propellant consists of particles of oxidizer (such as ammonium perchlorate) and aluminum in a polymeric matrix binder. The combustion products include H_2O, CO, CO_2, HCl, and N_2. There is little molecular oxygen in the products. Thus, the primary oxidizing compounds in aluminum combustion are believed to be H_2O and CO_2. The aluminum reacts to form primarily liquid Al_2O_3 with traces of gaseous aluminum hydroxides, chlorides. and sub-stoichiometric oxides.

The most widely studied problem in aluminum combustion in rocket motors is that of agglomeration (Price, et. al., 1982: Micheli and Schmidt. 1977). Because agglomeration is limited in the Rijke burner, it will not be addressed in this report.

5

3.2 Aluminum Ignition

Ignition can follow two potential pathways: (1) The destruction of the protective oxide coat to allow the aluminum to be exposed to the oxidizing atmosphere, or (2) the self-heating of the particle due to oxidizer diffusion through the oxide coat. The relative importance of these two pathways remains disputed. Research seems to indicate that the destruction of the metal oxide coat, rather than the self-heating, is the dominant mechanism. Generally for the aluminum particles studied in the Rijke burner (e.g. 10-60µm), the ignition temperature is believed to be in the range of 1700-2200° K (Friedman and Macek, 1962; Kuehl, 1965).

3.3 Basic Understanding of Aluminum Combustion

The combustion of aluminum has been found to be similar to liquid fuel droplet combustion. The reaction is believed to be limited by the diffusion of oxidizer towards the particle and the vaporized metal away from the particle. A flame zone develops at a distance of 1.5 to 4 radii from the particle surface where the oxidizer and vaporized metal meet and burn. The heat from the flame diffuses back to the surface to cause additional aluminum vaporization. However, unlike liquid fuels, aluminum combustion produces a condensed phase. This condensed phase oxide forms sub-micron particle smoke that surrounds the particle and forms a flame trail (Price, 1984b). Some of the aluminum oxide from the reaction products diffuse back to the particle surface and can be seen as bright islets (Razdobreev, et. al., 1976). The condensation of products on the surface of the particle provides additional energy which can increase the combustion rate of the particle (Law, 1973). However, the oxide cap reduces the surface area available for combustion and radiates heat away from the particle, slowing the reaction.

A complete understanding of aluminum combustion has been difficult for three reasons: (1) Combustion occurs around micron sized particles, burning within milliseconds, and under very harsh temperatures. (2) The combustion characteristics vary widely over experimental conditions. (3) The experimental data have not been reproduced using similar experimental techniques and conditions to assure validity of the individual data sets.

Most data have been correlated using the d-squared law, that is, the burn time is assumed to be proportional to the diameter of the original particle squared. Important assumptions involved in such an equation include steady-state behavior, spherical symmetry, and no reactions on the surface. In a limited number of cases, this law has been applied successfully; however, in general, burn time is proportional to the diameter raised to the 1.5 to 2.0 power. This discrepancy is probably due to experimental error, but several other explanations for the drop in exponent have been proposed. These include:

(1) Pokhil (1973) suggests that as pressure increases, the exponent drops.
(2) King (1977) has shown that finite kinetics could cause a drop in exponent.
(3) Law (1973) hypothesizes that the aluminum oxide covering reduces combustion rates of large particles.
(4) Kuo (1986) suggests convective effects as the primary cause for the exponential drop.

Russian authors have proposed a simple empirical burn rate law which allows for oxidizer concentration (Pokhil, 1973).

$$t_r = k \frac{d^{1.5}}{a_k^{0.9}} \qquad (3.1)$$

t_r is the reaction time, d is the diameter and a_k is the sum of the mole fraction of the oxidizers including O_2, H_2O, and CO_2. However, others (Micheli and Schmidt, 1977) believe that weighting all oxidizers equally is incorrect and propose that experimental evidence contradicts such practice.

3.4 Models

Several models have been proposed to describe aluminum combustion. The bulk of experimental evidence suggests that metal combustion is a vapor phase process. Brzustowski and Glassman (1964b) proposed one of the earliest models using many of the same features as hydrocarbon droplet models (See Glassman 1977). However, unlike droplet combustion, the aluminum flame temperature is fixed by the boiling point of the oxide and the condensed oxide effects the diffusion of the oxygen to the flame zone. Most later models were outgrowths of these original concepts. The salient assumptions involved in these models are outlined in Table 3.1.

Aluminum Combustion Models

Model	Radiation	Diffusion Thru Condensate	Flame Temp = f(oxide condens/dissoc)	Product Condensation on Surface	Condensed Build-up in Flame	Extended Condensation Zone	Kinetics of Al + CO2	Variable Properties	Multiple Oxidizers	Flame Temp = f(Oxidizers)	Flame Temp = f(Pressure)	Convective Effects
Brzustowski, 64	●	●	●									
Law, 73		●	●	●	●							
Law, 77		●	●	●	●	●						
King, 77							●					
Micheli, 79		●	●					●	●	●	●	
Kudryavtsev, 79		●				●					●	●
Gremyachkin, 79												●

Table 3.1
Aluminum Combustion Model Comparison

7

Law (1973) followed the work of Brzustowski including product diffusion to the particle surface and allowing for a wide range of experimental conditions. Later Law included an extended condensation zone (1974). However, this extended condensation zone was found to be important for low temperature surroundings only.

King (1977) relaxed the assumption that the kinetics of the reaction were infinite. Although the poor kinetic data used leaves the quantitative nature of the model in question, the exponent in the d^n burning law was predicted to be in the range of 1.35 to 1.90 for finite kinetics as compared to the value of 2.0 associated with infinite kinetics.

Micheli and Schmidt (1977) included the variation of properties in the zones surrounding the flame and effects of multiple oxidizing species including CO_2, H_2O, O_2, and Cl^-. Included in the model is the thermodynamic equilibrium of the reaction products and their corresponding heats of reaction. Rather than a closed form solution as in previous models, the diffusion and energy balances were integrated numerically in a stepwise manner allowing for varying properties and compositions.

The models do seem to predict the experimentally observed trends, at least qualitatively. Burn rate was found to be a strong function of oxidizer concentration and particle size, but is essentially independent of pressure which only enters into the equations through thermodynamic and transport properties.

3.5 Summary

Because empirical models can only be compared to experimental data over limited conditions fundamental models have also been proposed. Although each type of model explains certain observed phenomena, the bulk of the experimental evidence points to the validity of a vapor phase model. The description of aluminum combustion used in the original Raun Rijke acoustic model was based on a simple liquid droplet approach. In an effort to improve Raun's approach, several of the literature models have been investigated. Each of the models focused on different aspects of aluminum combustion. Rather than using only one of the literature models, this research combined many of the positive characteristics of these models together to create an improved approach.

4.0 PAST WORK DONE AT BRIGHAM YOUNG UNIVERSITY

Researchers at Brigham Young University have been studying various aspects of combustion instability as it applies to rocket motors for several years. Recent emphasis has been directed at the phenomenon of distributed combustion, utilizing a Rijke burner for experimental data. Most of this work has been reported previously n contract reports, literature publications and most recently in a review paper "A Review of Rijke Tubes, Rijke Burners and Related Devices" by Raun, Beckstead, Finlinson and Brooks in the journal, Progress in Combustion and Energy Science. Thus, this section will be very abbreviated.

4.1 Experimental Work

Braithewaite (1984a, 1984b) was the first student at Brigham Young University to study distributed combustion in the Rijke burner. He found that addition of burning particles of aluminum and zirconium carbide increased acoustic growth. The increase in acoustic growth was believed to be the result of energy addition by distributed combustion. Finlinson's research (1988) focused on characterizing the Rijke burner in terms of the gas properties and burner configuration. He studied the effects of various test parameters on acoustic growth rate. His results have been summarized in a series of publications (Finlinson, 1987,1988).

Barron (1991) continued with the work of Braithewaite using the improved experimental apparatus modified by Finlinson. He studied the acoustic growth rate with and without the addition of aluminum, zirconium carbide, and aluminum oxide particles. Similar to the work of Braithewaite, Barron found that 25 and 43 micron Al particles and 7 micron ZrC cause an increase in acoustic growth. However, unlike the work by Braithewaite, Barron found that 13 micron Al caused a decrease in acoustic growth at high concentrations.

4.2 Theoretical Work

In conjunction with the experimental work, a mathematical model of the Rijke burner was developed by Raun (1985) in order to aid in the analysis of data from the Rijke burner. This model predicts the mean properties as well as frequencies and acoustic growth rates in the Rijke burner. Unlike other Rijke models, Raun included particle combustion, particle/gas interactions, and varying gas temperature in the hot section of the burner. The Raun model appears to be physically realistic and describes the acoustic aspects of the Rijke burner quite well. A recent publication (Raun and Beckstead 1993) summarizes the approach in the model and the results obtained.

To model the flame response, Raun used a modified a flame transfer function from Bailey (1957). The propane flame ignition delay time and the derivative of the flame speed were the two parameters adjusted to fit experimental results. His results suggest that heat loss in the hot section, which had not been modeled previously, is of utmost importance in correctly modeling the acoustic growth.

Raun's Rijke model was also compared to the experimental results of Braithewaite using a simplified model of aluminum combustion from Glassman (1977) for liquid hydrocarbon droplet combustion. The model predicted an increase in acoustic growth due to the particles, however, the predicted values were an order of magnitude smaller than found experimentally. The current efforts have been directed at resolving this discrepancy.

9

5.0 STUDY OF THE ACOUSTIC-FLAME INTERACTION

A primary purpose of this current ork is to improve the mathematical model previously developed by Raun. The first phase of the Rijke model improvement is to determined the acoustic growth due to an acoustically active flame. The flame-acoustic interaction is the primary acoustic driving force in a Rijke burner, thus it must be understood before the secondary effects of such factors as aluminum distributed combustion can be properly quantified.

5.1 Advantages of the McIntosh Model

To improve the flame response model, several of the literature models discussed in Chapter 2 were investigated (See Table 5.1). Early models were based on simple transfer functions or simplified flame descriptions. while more recently, researchers have used large activation energy asymptotics. Of these more recent modeling attempts, the McIntosh model was found to be best suited to replace the revised Bailey transfer function originally used by Raun.

EARLY STUDIES

Property	Bailey	Merk	Jones
Date	1957	1957	1977
Approach Taken	Phenomenological	Phenomenological	Fundamental
Basis	1st Order Diff. Eq.	Transfer Function	Q in a Volume
Acoustics Studied	Yes	Yes	Yes
Easy to Build into Model	Yes	Yes	Yes
Problems:	Based on Observations	--	Poor Flame Description

LARGE ACTIVATION ENERGY ASYMPTOTIC STUDIES

Property	Buckmaster	Van Harten	McIntosh
Date	1983	1984	1983-90
Approach Taken	Fundamental	Fundamental	Fundamental
Flame Oscillation	LAEA	LAEA	LAEA
Acoustics Studied	No	Yes	Yes
Easy to Build into Model	No	No	Yes
Assumptions:			
Le	Le appr 1	Le appr 1	No bounds
Adiabatic	No	Close	No
Order of Reaction	1	1	2

Table 5.1
Comparison of Flame/Acoustic Interaction Models Available

In addition to the fundamental nature of the McIntosh model, it has several advantages over other recent flame models. First, the transfer function, although complex, contains relatively few unknowns. Most of the physical parameters can also be determined with reasonable accuracy. Only the flame holder impedance remains as an arbitrary unknown. Second, most of the assumptions used in this transfer function derivation are realistic. While other models assume an acoustic time much larger than diffusion time, small temperature changes across the flame, Lewis number close to one, and overall first order reaction rate, McIntosh relaxes these assumptions. Third, unlike many other flame models, McIntosh is actually studying a Rijke type device and his work compares qualitatively with the experimental work of Schimmer, et. al. (1977) and Rijke (1859).

5.2 Model Preparation

The McIntosh transfer function was coded, checked for correctness, and then included in the Raun Rijke acoustic model (See Appendix A for McIntosh transfer function description). This new Rijke model was tested by comparing its results to the work done by McIntosh. Although similar trends were obtained, the new Rijke model did not reproduce the results of McIntosh's original studies. This difference is attributed to certain dimensional parameters that required estimation in the Raun model because they were not explicitly defined by the non dimensional McIntosh model.

5.3 Model Parameter Determination for Experimental Comparison

The Rijke model parameters were determined using the data from Finlinson's studies, Edward's thermochemical program, and the McIntosh steady flame model. Since the Lewis number is associated with a single species but the model accounts for both fuel and oxidizer, Joulin and Mitani's "pseudo" lean species Lewis number model (1981) was used to correct the Lewis number for close to stoichiometric conditions. The corrected Lewis number can be determined from:

$$Le_c = Le_l + J(Le_r - Le_l) \tag{5.1}$$

where Le is the Lewis number and the subscripts c, l, and r represent the corrected, lean and rich species values, respectively. H is a parameter based on the equivalence ratio, activation energy, and temperature. (See Appendix A.)

Raun found that heat transfer from the gas in the hot section to the surroundings had a strong influence on acoustic growth. The constant heat transfer coefficient used in the original model was improved to more accurately account for these variations in temperature. The heat transfer in the hot section of the Rijke burner was modeled using an empirical correlation fit from complex numerical solutions for combined entry length and constant surface temperature:

$$Nu = c\left(\frac{Re \, Pr \, D}{x}\right)^{0.385} \tag{5.2}$$

11

(Shah and London, 1978). Values of the constant c used in the program were in the range of 1-2, consistent with the values of 1.1-1.3 found in fitting the original data. Linear perturbation analysis was also performed on the above equation to include in the model the effects of increased heat transfer due to acoustic oscillations.

Due to the sensitivity of the McIntosh transfer function on changes in flame temperature and flame holder impedance, these parameters must be predicted correctly in order to obtain acoustic growth values consistent with those seen experimentally. Because the values of these parameters are not well known, *a priori* acoustic growth determination is difficult. Instead, the flame temperature or flame holder impedance were adjusted to fit experimental acoustic growth values. The fitted values of acoustic impedance were compared to the work of Schimmer and Vortmeyer (1977). These researchers had a different burner configuration and flame holder than used in the Rijke burner, resulting in different acoustic impedance values. However, an order of magnitude comparison could be made between the experimental and computer fitted impedance.

5.4 Comparison with Experimental Data

The Rijke burner data from Finlinson used to verify both the McIntosh transfer function and Raun's Rijke model suffered from two experimental problems. First, the data sets showed large scatter and low reproducibility. Secondly, for any given experiment there was only a small operating range between where the flame would generate a detectable acoustic signal and where the acoustic signal became so large the cone could not damp it.

In the first experiment which was compared directly to the Rijke model, total mass flow rate was varied. As the mass flow increased, the acoustic growth rate increased until the frequency shifted to a higher harmonic and the growth rate dropped. (See Figure 5.1.) The flame temperature in the model was varied to permit the acoustic growth rate to fit the experimental data. A good fit with less than a 10% error in acoustic growth and less than 2% error in the frequency was obtained. The fitted flame temperature was found to increase in a somewhat linear fashion, similar to the temperature determined by the experimental work of Finlinson.

Another set of experimental data fitted with the Rijke model was obtained to determine the effect of variable cold length on acoustic growth and frequency. The cold length was varied with the gas proportions and velocity remaining constant. A complex relationship between acoustic growth and cold length was found from the experiment (See Figure 5.2). The fitted acoustic growth rate fell within experimental scatter while the frequency was within 10% error or less. In the model, the flame holder impedance rather than temperature was varied to fit the experimental data since temperature should remain constant for all cases and impedance varies with frequency. In determining if the values of impedance are plausible, they were compared with the Schimmer and Vortmeyer data (1977). Although their burner configuration was quite different, the fitted impedance from the Rijke model followed somewhat similar trends and changed sign at nearly the same frequency as their experimental work.
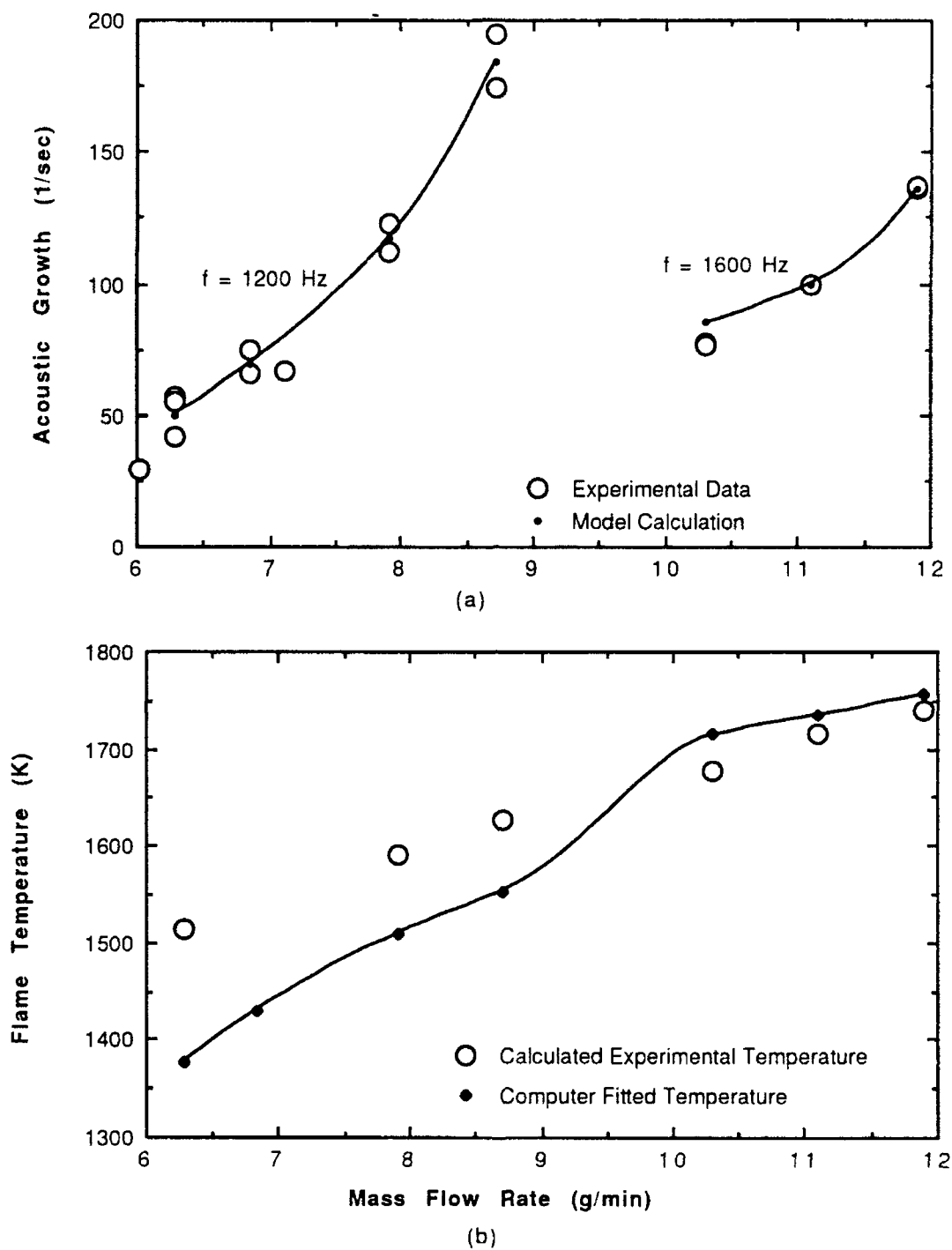
Figure 5.1 Comparison of Rijke model and Experimental (a) Acoustic Growth and (b) Flame temperature for varying mass flow rates.
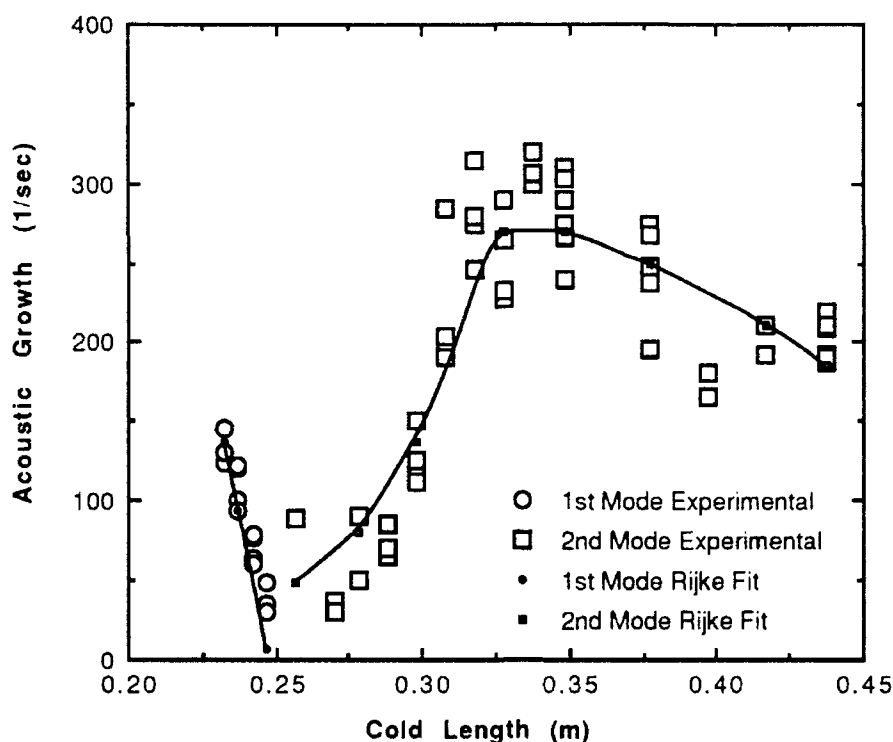
Figure 5.2 Comparison of Rijke model and experimentally determined acoustic growth for varying cold section.

Because the temperature in the Rijke burner determines the speed of sound and in turn the frequency, frequency is an independent method of determining the accuracy of the temperature profile and the flame temperature. The calculated frequency for the previously presented data fit the experimental values within 10% in all cases. Such a fit suggests that the flame temperature values and the heat transfer correlation used to fit the data are reasonable.

5.5 Discussion of Experimental Comparison

Not only should there be a coherent relationship between fitted flame temperatures of a single experiment, but also a coherent relationship between the data for all experiments. In Figure 5.3, the adiabatic flame temperatures for similar tests are compared to their respective model fitted flame temperatures. Although there is some variation between experiments, there is a general upward trend in all the data. The figure also shows a difference nearly 1000 °K between the adiabatic and actual flame temperature, indicating that the flame is highly non adiabatic. Similarly, Finlinson found differences of approximately 800° K between the adiabatic and actual flame temperature. This decrease in flame temperature is believed to be due to heat conduction back to the flame holder, soot radiation, and heat removed by the cooling jacket.
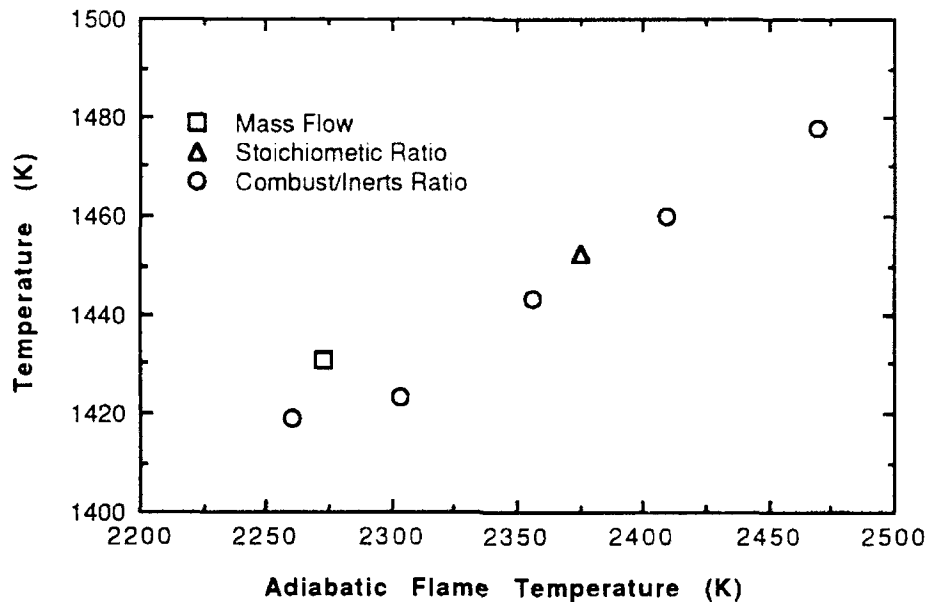
Figure 5.3 Comparison of fitted flame temperature and adiabatic flame temperature for similar test cases.

5.6 Summary

The McIntosh transfer function for the flame is believed to be an improvement over the Bailey model originally used by Raun in the following ways. McIntosh's model has its advantage in that it is based on conservation equations and known flame structure. It does seem to fit the data fairly well with only three parameters being adjusted: flame temperature, flame holder impedance, and the constant used in the heat transfer equation. The values of these properties in general are reasonable. Furthermore, there does appear to be good physical basis for the response of the transfer function rather than being solely an empirical curve fit.

In spite of these advantages, *a priori* acoustic growth determination remains elusive due to: (1) the difficulty in accurately determining the model properties, many of which are not well defined (e.g. temperature); and, (2) the incorrect assumptions made in the model derivations which would require that known parameters be adjusted outside of the expected range.

The modified Rijke model fits the data quite well. The complex trends associated with Finlinson's data can be followed, indicating a degree of fundamental correctness of the model. This model as it stands has been used in studying distributed combustion.

15

6.0 ALUMINUM COMBUSTION MODEL DERIVATION

6.1 Law's Aluminum Combustion Model

The model by C. K. Law (1973) was used as a backbone for the current work because it conformed to the following criteria. First, Law's model uses an analytical solution rather than a numerical one. Because the aluminum combustion model is only a single module of a larger computer code which is accessed hundreds of times, the increase in computer time required for a numerically integrated particle burn model would be immense. Second, his model is based on physically realistic parameters as input most of which are known (e.g. densities, boiling points, diffusivities, heat capacities, etc.). Third, the model describes the majority of the experimentally observed behavior, including a vapor phase diffusion flame and surface formation of aluminum oxide. Lastly, the derivation is straight forward, allowing easy modification.

The Law model is a diffusion-limited vapor phase combustion model. The conservation equations of energy and species, respectively are used in its derivation are shown below (See the Appendix for complete details).

$$\frac{\partial}{\partial t}\rho H = -\left(\nabla \cdot \rho \vec{v} H\right) - \left(\nabla \cdot \vec{q}\right) - \left(\tau : \nabla \vec{v}\right) + \frac{Dp}{Dt} + Q_r \tag{6.1}$$

$$\frac{\partial}{\partial t}\rho_i = -\left(\nabla \cdot \{\rho_i \vec{v} + \vec{j_i}\}\right) + r_i \tag{6.2}$$

Assumptions of the model include:

1. Pseudo-steady state burning
2. Spherically symmetric burning
3. Negligible viscous forces
4. Isobaric conditions
5. Diffusion flame with infinitely thin reaction zone
6. Negligible volume fraction of the oxide smoke
7. Burning aluminum particles are at their boiling points
8. Fick's and Fourier's laws

After integration and application of the boundary conditions at the flame, the equations of energy and species take on the form:

$$\dot{m}\left(r^{-1} - r_f^{-1}\right) = -4\pi\rho_g D_i \ln\left\{1 - \frac{\dot{m}C_p(T_f - T)}{\dot{m}C_p(T_f - T_s) - \dot{m}_c Q - \dot{m}_v Q_1 - H}\right\} \tag{6.3}$$

$$\dot{m}\left(r^{-1} - r_f^{-1}\right) = 4\pi\rho_g D_i \ln\left\{\frac{\dot{m}Y_{i,f} - \dot{m}_i}{\dot{m}Y_i - \dot{m}_i}\right\} \tag{6.4}$$

for both the regions between the particle and the flame and the flame and infinity. The mass fluxes of reactants and products are determined by stoichiometry and the heat flux H determined from the conditions at the particle surface. These equations can then be combined and the mass flux, $\dot{m}$, removed from the solution. The ratio of condensed to vaporized oxide or the flame temperature is determined in the course of solution of these equations. Once a solution is obtained, the mass flux of aluminum can be calculated and the burn time determined.

Unlike other similar models, Law includes the effects of product diffusion to the surface of the particle. Law also makes an effort to account for the directions of bulk flow, as they are responsible for the motion of the condensed phase oxide product. Four potential modes of burning are possible, based on the temperature and composition of the surrounding gas. (See Figure 6.1 and Table 6.1)
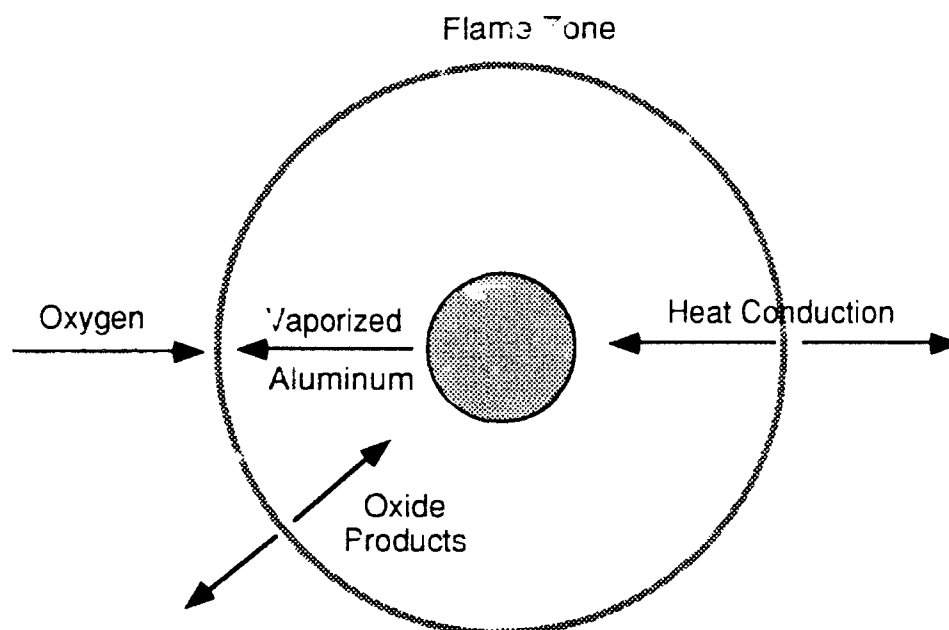
Figure 6.1 Schematic of Law's aluminum combustion model .

Table 6.1
Modes of Aluminum Combustion

| Gas Temperature or Oxidizer Concentration	Flow Direction		Flame Temperature	Fraction of Oxide Vaporized
	Between Flame and Particle	Between Flame and Infinity		
Low	Outward	Inward	< T boil	0
Medium	Outward	Inward	at T boil	0-1
Medium	Outward	Outward	at T boil	0-1
High	Outward	Outward	> T boil	1

17

At low gas temperature or oxidizer concentration, the motion of the gas is toward the flame and the flame temperature is below the boiling point of the oxide. With increased temperature or oxidizer concentration, the flame temperature reaches the boiling point of the oxide and the fraction of vaporized oxide begins to increase. Higher quantities of vaporized oxide result in an increase in diffusion of matter away from the flame and the gas flow between the flame and infinity switches directions. At high gas temperature or oxidizer concentration, all the oxide is vaporized and the flame temperature once again rises with increased concentration or surroundings temperature.

6.2 Improvements to the Law Model

This work is an effort to improve the original Rijke model by (1) making it more applicable to the Rijke burner and (2) relaxing assumptions which might be unreasonable. However, no additional complications were added which would require numerical solution of a differential equation. The improvements are tabulated in Table 6.2. Schematics of the features included in the model developed in this study are shown in Figure 6.2.

Table 6.2
Comparison of Original Law Model and Improved Model

Assumptions of the Original Law Model	Assumptions of the Improved Model
1. Properties Constant everywhere	Calculation of properties based on weighted average of properties at particle surface, flame and infinity.
2. Oxygen only reactant	Multiple species allowed with variable transport and thermodynamic properties.
3. Burning in Stagnant Gas	Accounts for convective effects based on the Nusselt number.
4. Radiation neglected	Accounts for radiation between particle, flame, and surroundings.
4. Lewis Number = 1	Allows Lewis numbers different than 1.
6. Oxide on particle surface has no effect.	Reduced burn rate due to oxide surface coverage.

18
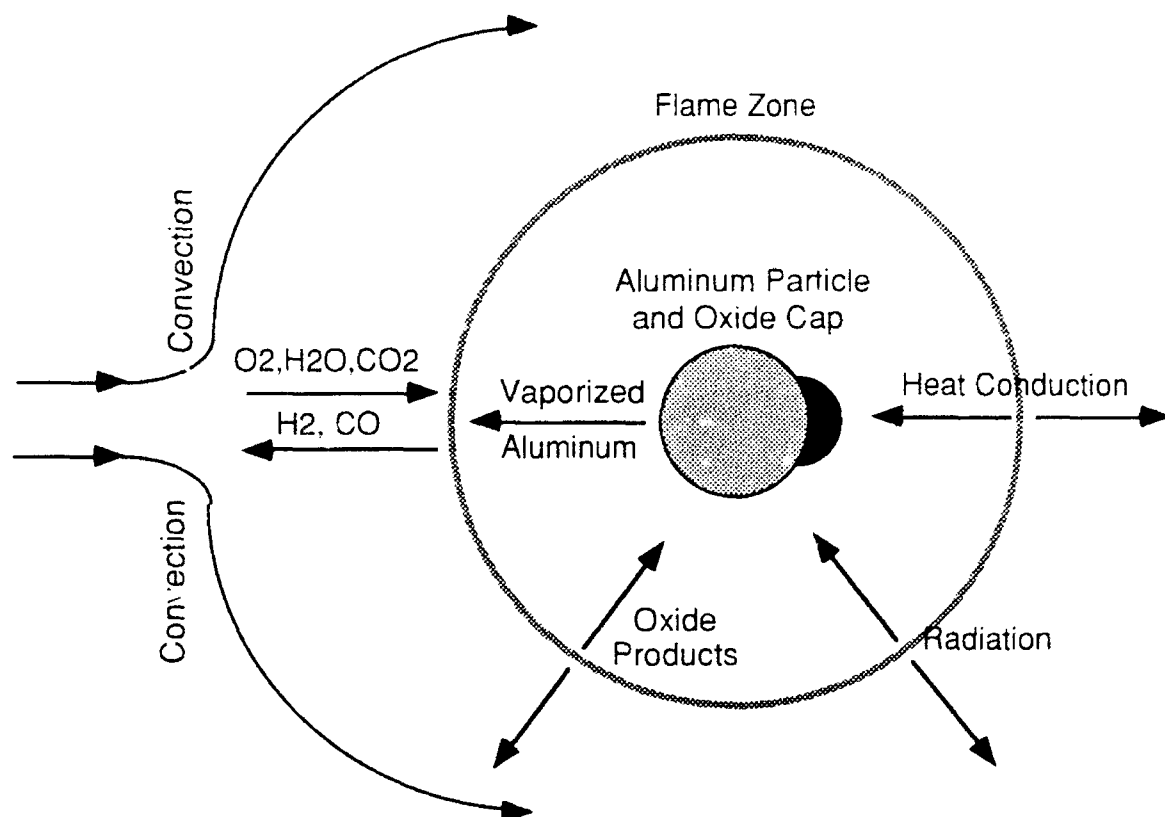
Figure 6.2 Schematic of aluminum combustion model used in this study.

6.2.1 Variable Properties/Oxidizers

To achieve an analytical expression, the integration of the heat and species equations assumes constant properties in the regions between the particle and the flame (Region A) and between the flame and infinity (Region B). Averaged transport properties are determined for these regions, by weighting the properties at the particle surface (s), flame (f) and at infinity (∞) according to (Chung and Law ,1984):

$$\phi_{A,B} = \frac{1}{w+1}\left(\phi_{s,f}\, w + \phi_{f,\infty}\right) \tag{6.5}$$

where ϕ is any given transport property. A value of 2 is used for the weighting factor w as suggested by Chung and Law. These property values are allowed to vary throughout the solution as the concentration of the gaseous species vary during the combustion process. In addition, the Lewis number is not constrained to unity.

Finally, the improved model allows for multiple oxidizers including water, carbon dioxide, and oxygen, since all three are present in both the Rijke burner and in propellant exhaust gases.

6.2.2 Heat and Mass Transfer Effects

Convection effects were accounted for using a simplified technique originally suggested by Frank-Kamenetski (1969) known as the "reduced-film" approximation (Gremyachkin, 1979). This approximation consists of choosing some "region of influence" around the particle in which the change in temperature and concentration

19

occurs. Outside this layer, the temperature and concentrations are assumed to be at the bulk value. This approach works reasonably well for the steady-state modeling of aluminum; however, it should be noted that it does not describe the characteristics of fluctuating aluminum combustion.

Heat transfer by radiation is treated solely as gray-body emissivity between the flame and the particle surface and the flame and the surroundings. The oxide smoke, not the gaseous flame, is responsible for the majority of the radiation from the flame to the particle surface. Determining the optical thickness of the oxide smoke has not been addressed in this study.

6.2.3 Oxide Build-Up on the Particle Surface

Finally, an understanding of the condensed oxide on the surface of the particle has been considered important by many experimentalists (e.g. Prentice, 1974; Razdobreev, 1976; Hunter, 1965). In order to account for the change in combustion rate due to surface coverage of condensed aluminum oxide, the burn rate is proportioned according to the surface area covered by the oxide to the surface area if no oxide were present. According to pictures taken of partially burned particles, the aluminum and oxide "cap" can be approximated as fractions of spheres attached together. The smaller particle is assumed to be a half-sphere, while the large particle is assumed to be a partial sphere having a radius:

$$r = \frac{a^2 + h^2}{2h} \tag{6.7}$$

where a is the radius of the smaller particle, V is the volume of the larger particle and h can be defined as:

$$\frac{6}{\pi} V h^3 - 3a^4h^2 - a^6 = 0 \tag{6.8}$$

Using these equations, the changing surface area of the aluminum due to the build up of the oxide cap can be more correctly accounted for.

7.0 RESULTS OF THE STEADY STATE ALUMINUM MODEL

This section discusses the model sensitivity analysis and makes comparisons to experimental results.

7.1 Effect of Particle Diameter

Figure 7.1 show the calculated particle diameter as a function of time. Initially, the particle does not have an oxide cap to inhibit burning, so that the particle burns across the entire surface. However, as oxide accumulates, the burn rate slows due to the decreased surface area. The predicted instantaneous burn rate appears to be

better correlated by a $d^{1.5}$ law, due to the variation in surface area caused by the oxide accumulation.
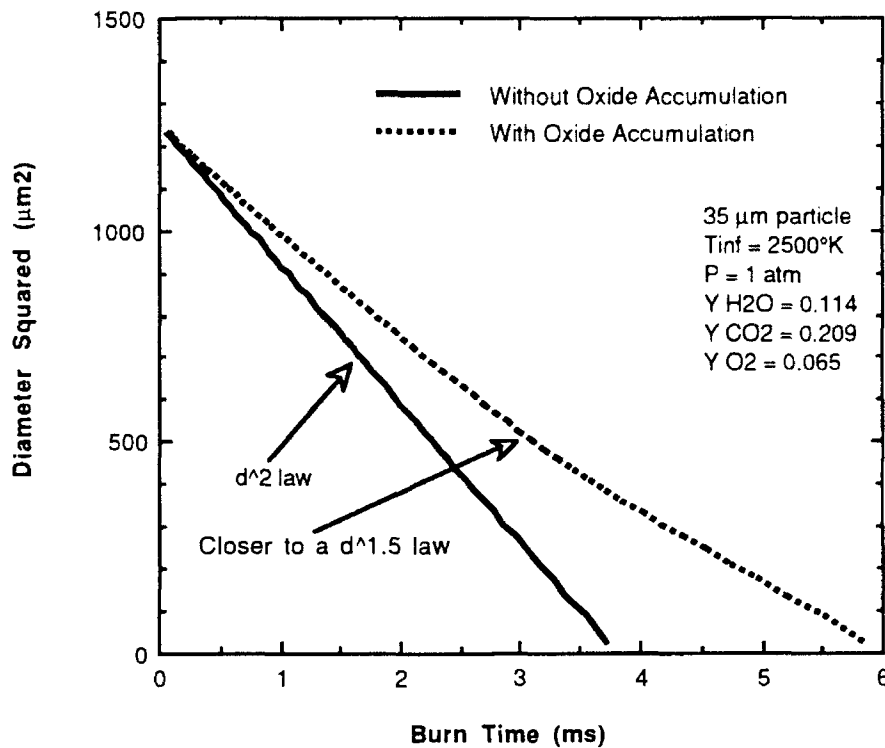
Figure 7.1 Effect of Oxide Accumulation the Particle Surface.

7.2 Effect of Concentration

7.2.1 Influence on Burning Rate.

It has been suggested by numerous experimentalists that the burn time is inversely proportional to the oxidizer concentration (e.g. Davis, 1963). A sensitivity analysis of the model showed that for a given oxidizer this is true. However, the proportionality constant between burn rate and individual oxidizers is not constant. Each oxidizer has a different effect on the burn rate.

The Russian empirical correlation (Equation 3.1) suggests that the burn rate is proportional to the total oxidizer mole fraction to the 0.9 power. Using the model to test this correlation it was found that each of the oxidizers have differing effects on the burn time and cannot simply be summed together. The simple Russian correlation can not account for the variation in heats of reaction, transport properties, and products formed from oxidizer to oxidizer.

A more appropriate correlation appears to be

$$t_b = C \frac{d^2}{\sum c_i x_i}$$

(7.1)

21

where C is a constant based on ambient temperature and pressure and c_i and x_i are the constants and mole fractions for the individual oxidizing species, respectively. The concentration of one species at a time was varied over a range of approximately 200%. For conditions similar to those found in the Rijke burner, the values of c_i for H_2O, CO_2, and O_2 were calculated from Figure 7.2 to be 0.533, 0.135 and 1.0, respectively.
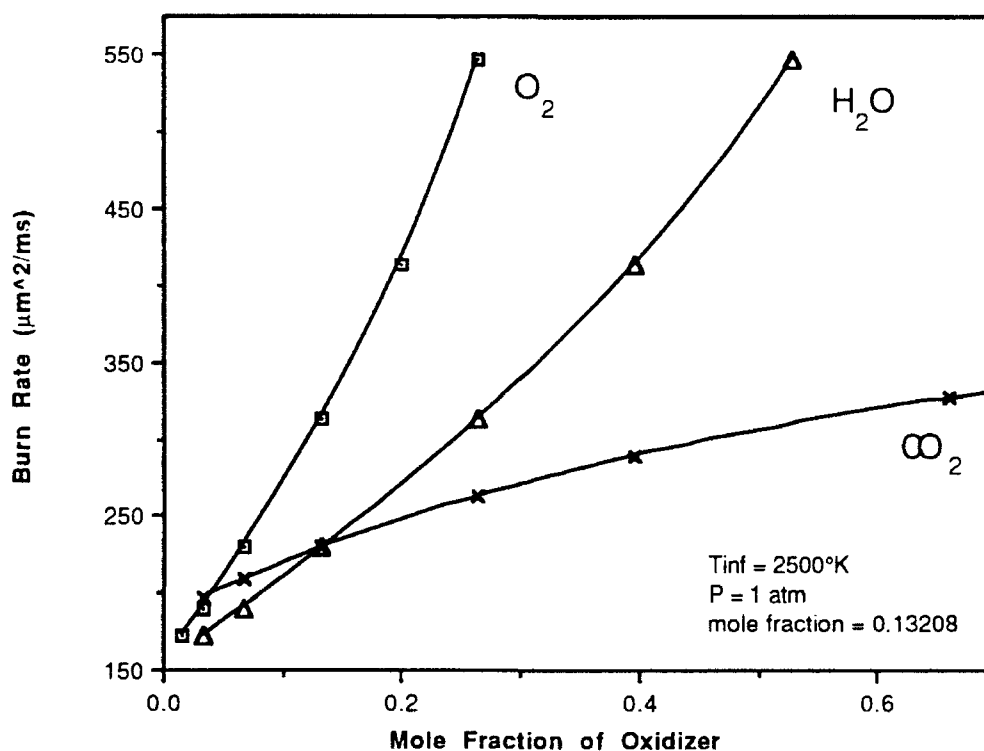

Figure 7.2 Calculated aluminum burn rates showing the effect of oxidizer concentration, holding the other two species constant.

Oxygen has approximately twice the oxidizing capabilities as water and seven times the oxidizing capabilities of carbon dioxide. If the above constants are normalized with respect to the heat of reaction times the diffusivity divided by the molecular weight of the individual species, the oxidizer effects become nearly equal. This result stems from oxygen having twice as much oxidizer per mole and a higher heat of reaction. Water and carbon dioxide have comparable heats of reaction, but water has a lower molecular weight and a higher diffusivity. Carbon dioxide has only a marginal effect as an oxidizer.

7.2.2 Influence on Flame Standoff Distance

The flame standoff was also investigated with respect to oxidizer concentration. It was found that for conditions similar to the Rijke burner, the flame radius increases with the addition of oxygen and decreases with the addition of water and carbon dioxide (See Figure 7.3). These results are similar qualitatively to numerous experimental investigators (e.g. Pokhil, 1973, Wilson and Williams, 1971). The predicted changes, however, are not as large as those seen experimentally (e.g. a

flame radius of 1.5 for atmospheres with water and a flame radius of 3 for those in oxygen).
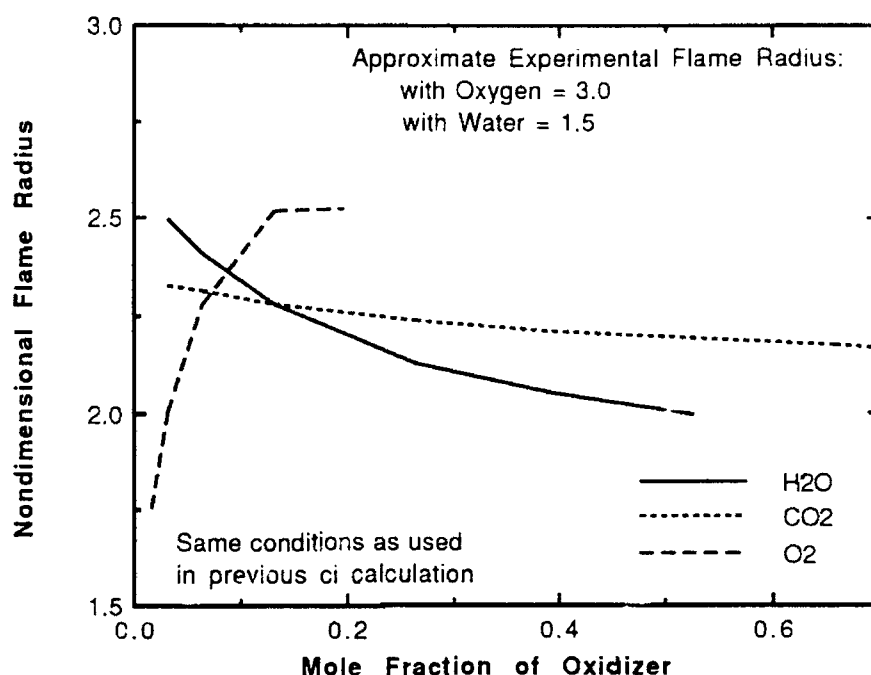
Figure 7.3 Calculated flame standoff distance as a function of oxidizer concentration.

7.3 Effect of the SurroundingsTemperature

The effect of the temperature of the surrounding gas was also investigated with the model. An increase in ambient temperature resulted in an essentially linear increase in burn rate when the flame temperature is lower than the boiling point of oxide. However, if the flame temperature reaches the oxide boiling temperature (at approximately 1500°K) the slope of the curve increases slightly.

7.4 Flow Field Effects

The effect of the particle being immersed in a flow field was investigated. In the model, the burn time is not effected by convection until the Nusselt number is greater than 2.1. For larger Nusselt numbers, both the burn time and the flame radius decrease. Kuo (1986) has suggested that in high flow conditions, the burn rate is changed from a d^2 law to a $d^{1.5}$ law due to convective effects. This result stems from the fact that for a sphere, tne Nusselt number can be represented as

$$Nu = 2 + cRe^{0.5} \tag{7.2}$$

As the Reynolds number gets very large. the Reynolds number dominates the value of the Nusselt number. The $d^{0.5}$ in the Reynolds number then causes the exponent in the burn time to drop to 1.5. As the Reynolds number approaches infinity, the equations in this model also give the same result. However, using Reynolds numbers up to 25, the

23

burn time correlation was found to only drop to $d^{1.88}$ due to the convective flow. It was not possible to simulate higher flows due to convergence difficulties.

7.5 Additional Parameters Investigated

Several parameters in the model are not well quantified. Table 7.1 shows the relative effect of each of these parameters for the same conditions as shown in Figure 7.3.

### Table 7.1
Effect of Various Parameters on Burn Time

Parameter	Range Studied	Effect on Burn Time
1. Radiation	$0 < \varepsilon < 1$	-5 to -15%
2. Weighting Factor	$0 < w < \infty$	50%
3. Heat of Vaporization	50%	-25%
4. Heats of Reaction	pos/neg	15%
5. Diffusion to Surface	yes/no	-40%
6. Oxide Accumulation on surface	yes/no	25%

We will now look at each of these parameters.

1. Radiation: For small particles (< 40 μm), radiation between the aluminum particles and the condensed oxide at the flame has little effect over the entire range of emissivities from zero to one. For particles 50-100 μm and a flame emissivity of one, radiation of the flame has a larger effect (e.g. 10-20%). Realistically, the emissivity of the flame only becomes large when oxide has accumulated in the flame zone. This will occur when the particle is near burnout and is small. Thus, radiation should actually have little effect on the overall burn time.

2. Transport Property Weighting Factor (Eq'n 6.5): By weighting the properties either totally by the conditions at the flame or totally by the conditions at the particle surface and infinity, a maximum 50% change in burn rate results.

3. Heat of Vaporization: It has been postulated that the surface oxide reacts with the aluminum to form suboxides which leave the particle surface, thus complicating the value of the heat of vaporization (Gremyachkin, 1975).

$$Al_2O_3(l) + Al(l) \longrightarrow Al(g) + Al_2O(g) + AlO(g) \qquad (7.3)$$
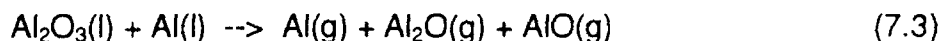
To account for this change the heat of vaporization was varied to determine its effect and found to be significant.

4. Heats of Reaction: The heat of reaction associated with the aluminum reacting to form vaporized oxide has been postulated by Law to be exothermic, however, thermodynamic calculations indicate that the reaction may in fact be endothermic. An endothermic heat of reaction seems most reasonable. Changes in this parameter also result in changes in heat transfer to the surroundings.

24

5. Diffusion to Surface: The diffusion of oxide to the surface may increase the reaction rate by as much as 45% due to the increased heat release from oxide condensation on the surface.

6. Oxide Accumulation on Surface: The oxide accumulation on the particle surface slows the reaction by approximately 25% due to surface coverage.

7.6 Comparison To Experimental Results

The model was compared to experimental results from several sources to determine its accuracy and versatility. Calculations were made for each data set considering the two extremes: (1) oxide diffuses back to the surface and its condensation provides energy to the particle, resulting in increased reaction rate; (2) oxide on the surface forms a cap, reducing the effective reaction area, thus slowing burning.

7.6.1 Burner Data

Studies where the aluminum that was ignited in gas burners is certainly the most applicable to the work done in the Rijke burner at Brigham Young University. Experimental results are taken from Friedman and Macek (1962,1963; Macek, 1967) and are compared to the model calculations in Figure 7.4.
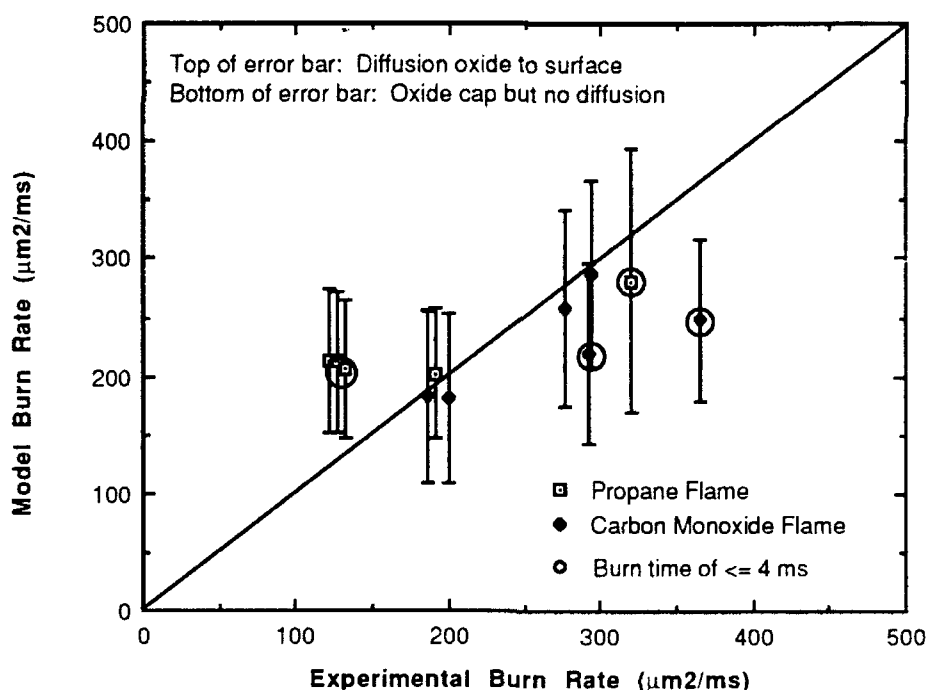
Figure 7.4 Comparison of model to experimental results for the burner generated data.

The larger value associated with the top of the error bars represents the calculation in which there is diffusion of oxide back to the surface of the particle and no oxide cap forms. The smaller value associated with the bottom of the error bars

represents the calculation in which there is no diffusion of oxide back to the surface of the particle and surface oxide accumulation occurs.

The model generally compares very well to the experimental results. Most of the disagreement is believed to be associated with small particles burning very rapidly (e.g. ≤ 4 ms, the circled datum points). Error in these data probably stems from experimental difficulties in measuring short burn times. The error associated the other two outliers has not been totally explained. Two potentially key elements in determining the cause are: (1) these are the only two data points taken from the 1963 experimental work of Friedman and Macek, and (2) these tests were performed at higher concentrations of water than other experiments in this data set.

7.6.2 Laser-ignited Data

The aluminum combustion data for particles ignited in a chamber with a laser comes from the work of Prentice (1974) and Wilson and Williams (1971). The data were taken at lower temperatures and generally higher oxygen concentrations. Primary oxidizers include oxygen and carbon dioxide. Only traces of water vapor were present. Only data taken at oxygen concentrations lower than 30% were used to reduce the effects due to fragmentation which occurs at higher oxygen concentrations.

Results of the comparison are shown in Figure 7.5. The upper portion of the error bar seems to fit the data best. The upper error bar is associated with diffusion of metal oxide back to the surface without oxide accumulation.
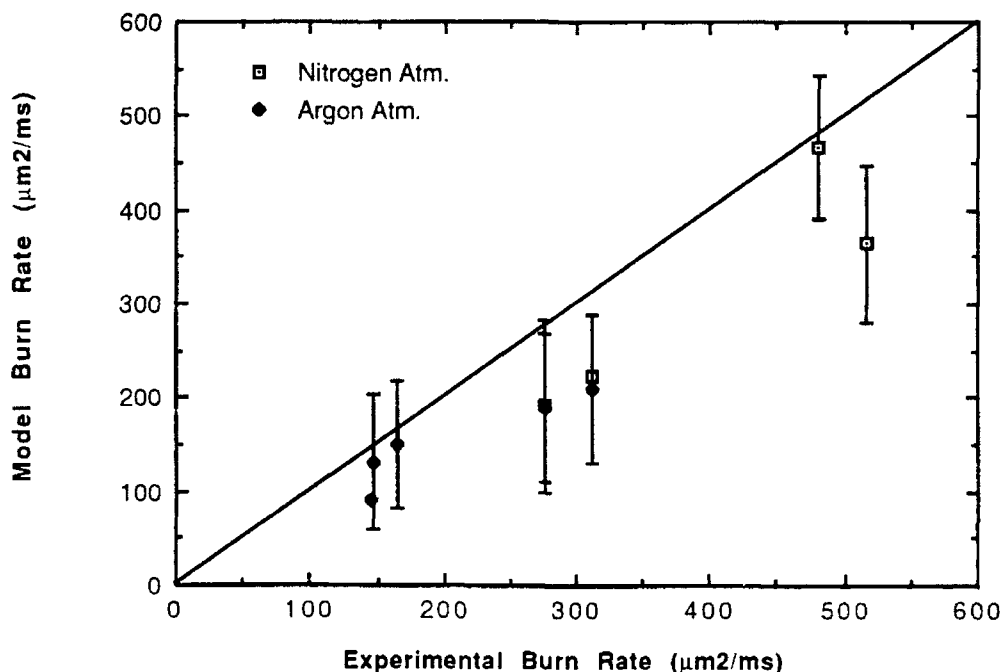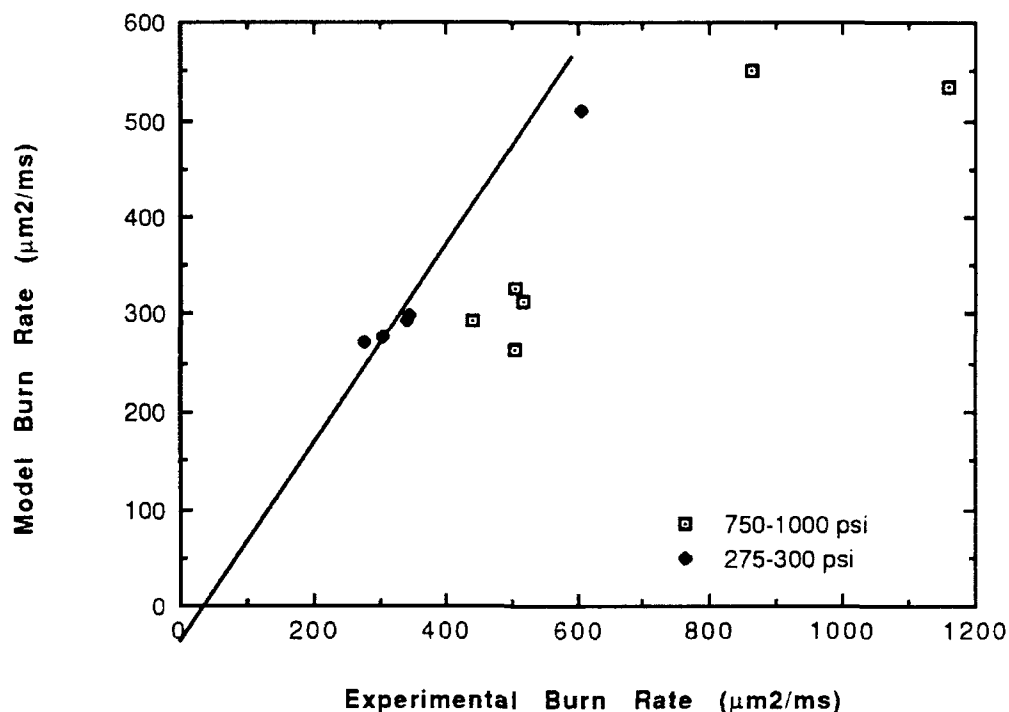

Figure 7.5 Comparison of model with experiment for laser-ignited aluminum combustion.

7.6.3 Propellant Data

Propellant experiments performed by Davis (1963) and Hartman (1971) provided the third data set. Their work was done both at a low pressure (275-300 psi) and a high pressure (750-1000 psi). For the low pressure data, the model follows

26

experimental trends reasonably well. However, at high pressure, the experimental results indicate a substantial increase in burn rate which the model does not predict. (See Figure 7.6.)

Figure 7.6 Comparison of Model with Experiment for Propellant data.

Pressure only enters the model in the temperature dependent properties associated with increased particle and flame temperature. For this reason, the model only predicts a 20% increase in burn rate over the range of 14 to 1000 psia; much lower than apparently observed experimentally. Further work is needed to determine the pressure effect.

8.0 STUDY OF THE RIJKE MODEL

A primary purpose of this research is to understand the characteristics of the acoustics in the Rijke burner both with and without aluminum combustion. The first phase of this work was to understand the process of aluminum combustion without transient influences of an acoustic wave. The second phase was to understand the transient influences of aluminum combustion on an acoustic wave. The analysis of the Rijke acoustic model with the incorporation of the aluminum combustion model will be divided into a description of the mean property calculation and the acoustic property calculation.

27

8.1 Mean Properties in The Rijke Burner

The Raun Rijke acoustic model is divided into the solution of mean and oscillatory conservation equations. Mean properties do not vary with time and are solely a function of location in the burner. Oscillatory properties describe the acoustics in the burner and are a function of location in the burner and the frequency and acoustic growth. Solution of the equations describing the oscillatory properties in the burner require first a knowledge of the variations in mean properties of the gas and the particles in the hot section. In order to obtain profiles of these mean properties, the location and rate of aluminum combustion must also be known.

8.1.1 Ignition Delay

Where the particle ignites is important to properly calculating mean properties. The original Raun Rijke acoustic model assumed that the particles are in thermal and velocity equilibrium with the gas immediately after passing through the flame, thus not allowing for particle acceleration and heat-up. In the current work, the terms responsible for particle convection of momentum and energy

$$\rho_p v_p \frac{\partial v_p}{\partial x} \text{ and } \rho_p v_p \frac{\partial h_p}{\partial x} \qquad (8.1)$$

were reintroduced into the continuity equations to allow for the influence of acceleration on ignition delay. Ignition is assumed to occur when the particles reach some specified temperature.

The assumed ignition temperature in the simple model was adjusted until ignition delay times were matched to the experimental work of Friedman and Macek (1962) and Davis (1963). Since the melting point of aluminum oxide is ~2300°K, considering thermal stresses during heat-up, values in the range of 1600-2300°K were considered. The best fit of the experimental data occurs with an ignition temperature of approximately 1900°K. Using values of 1600 resulted in calculated ignition delay times approximately 30% low while values of 2300 resulted in values ~30% high. Thus, the value of 1900 was used in all other calculations in the Rijke acoustic model to determine the location of aluminum ignition in the burner.

This study compared ignition delay results of the Rijke acoustic program to the solution of simple stand-alone computer models. Equations describing both the energy and momentum of a single particle were solved in order to determine if the step size of the Runge-Kutta calculation was sufficiently small to properly calculate ignition delay. The results of the Rijke program were found to differ by less than 5% from the results of the simple model for particles in the range of 15 to 65 μm in diameter.

8.1.2 Aluminum Combustion Model

All of the features of the aluminum combustion model described previously, were incorporated into the Rijke acoustic model. To assure proper coding of the aluminum combustion portion of the model, the results of the Rijke program were compared to the stand-alone aluminum model. Differences of less than 5% were determined. Remaining error is believed to be associated with the Runge-Kutta numerical routine.

Within the model heat transfer can occur between phases in the following ways: (1) convective heat transfer between the particles and the gas, (2) radiation between

the particles and the surroundings, (3) production of heat due to the reaction of aluminum with its oxidizer, and (4) heat loss from the gases to the surroundings. A calculated gas temperature profile is shown in Figure 8.1. In most respects the curves follow expected trends. However, for values of oxide emissivity greater than 10%, the outlet gas temperature with aluminum addition is actually lower than the case with gas only. It appears that heat from the gas is convected to the oxide particles and then expelled to the surroundings as radiatic
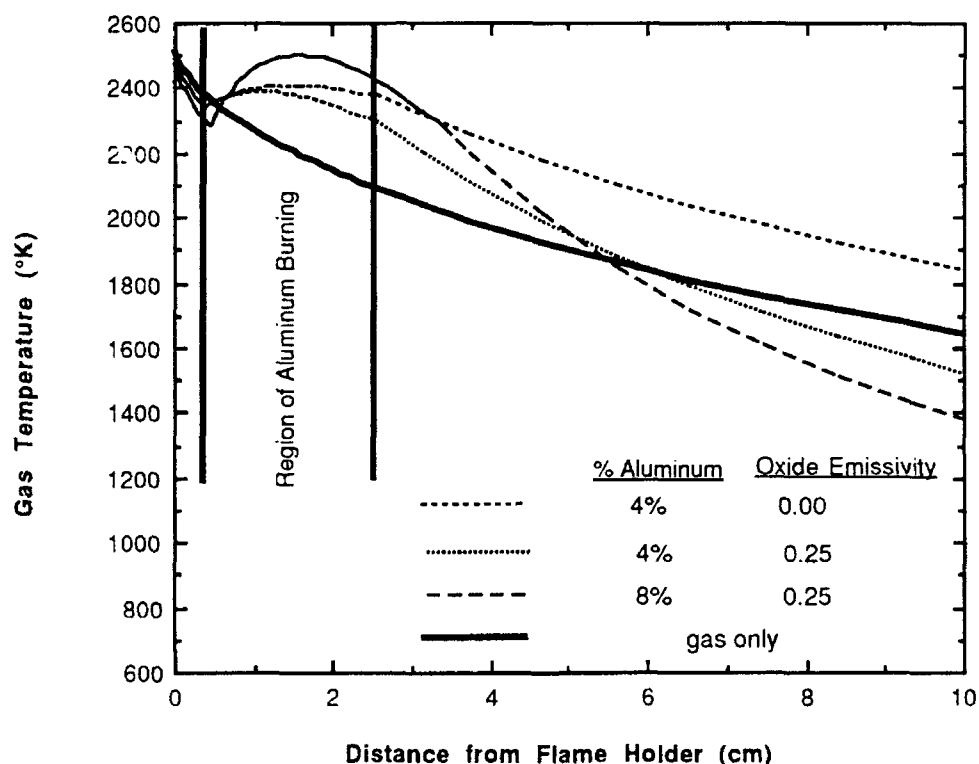
Figure 8.1 Gas temperature for 25μm aluminum particle for various emissivities and percentages aluminum.

8.2 Acoustic Properties in the Rijke Burner

In the original Rijke program, Raun used a linear perturbation of a liquid droplet combustion model to describe the fluctuating particle reaction rate. His acoustic growth rates for an acoustically inactive burner flame were an order of magnitude lower than those observed experimentally by Braithewaite. These results provides motivation for the current modeling work.

8.2.1 Early Rijke Model Development in this Work

Similar to Raun s work, calculation of the fluctuating aluminum reaction rate in this work uses a linear perturbation equation:

$$\hat{r}_p = \frac{\partial r_p}{\partial T_g}\hat{T}_g + \frac{\partial r_p}{\partial p}\hat{p} + \frac{\partial r_p}{\partial p_p}\hat{p}_p + \frac{\partial r_p}{\partial v_g}\hat{v}_g \qquad (8.2)$$

29

where the derivatives of the particle reaction rate r_p are calculated numerically from the improved aluminum combustion model, rather than from a simple liquid droplet model as done by Raun. Once again the acoustic growth rates calculated with the improved model were an order of magnitude lower than those seen experimentally. Subsequently, three reasons for the discrepancy were examined: (1) Incorrect form of the particle reaction rate equations; (2) Incorrect interactions between the particle reaction model and other parts of the Rijke model calculation; and (3) Limiting assumptions of perturbation theory.

8.2.2 Form of the Particle Reaction Rate Equation

Difficulty in fitting experimental data could be the result of an incorrect form of the particle reaction rate equation. Both Raun's Rijke model and the one of this study assume the reaction rate is limited by the diffusion of reactants to the flame front. As suggested by King (1977), the reaction rate could instead be limited by the kinetics of the reaction. To test such a conjecture, the particle reaction rate was assumed to be an Arrhenius function of the surface temperature. For reasonable values of the order of the reaction (n = 2) and the activation energy (E_a = 40,000 cal/mole), the values of the reaction rate continued to be an order of magnitude too small, suggesting that the form of the equation is not the primary reason for the discrepancy between the model and experiment.

To determine the magnitude of the parameters required to produce the proper results, an empirical fluctuating reaction rate equation of the form:

$$\hat{r}_p = \left(\Psi_p \hat{p} + \Psi_v \hat{v}_g\right) \bar{r}_p \qquad (8.5)$$

(where Ψ is an arbitrary complex constant) was studied with regards to distributed combustion. Calculated acoustic growths of the proper magnitude could be achieved with this type of expression. Values of the pressure dependent complex constant would have to be primarily real and on the order of 10^{-3}. Values of the velocity dependent complex constant would have to be primarily imaginary and on the order of 1. These results suggest that the fluctuating reaction rate must be in phase with the pressure and 90° out of phase with the acoustic velocity, similar to what would be expected by the Rayleigh criteria.

8.2.3 Interactions between the Particle Reaction and the Rijke Burner Flame

Difficulty in fitting experimental data could be due to improper descriptions of the relationships between the particle reaction rate and other parts of the Rijke acoustic model. To evaluate this idea, the revised Bailey flame model (as used by Raun) was used to make parametric calculations. It was found an increase in acoustic growth (See Figure 8.2) of similar magnitude to that seen in experimental work was calculated, in spite of the fact that the fluctuating aluminum combustion terms in these calculations were set to zero. This surprising result seems to indicate that the addition of aluminum changes the mean properties of the burner sufficiently to cause changes in the propane flame response without the need for the fluctuating heat release due to the particles.
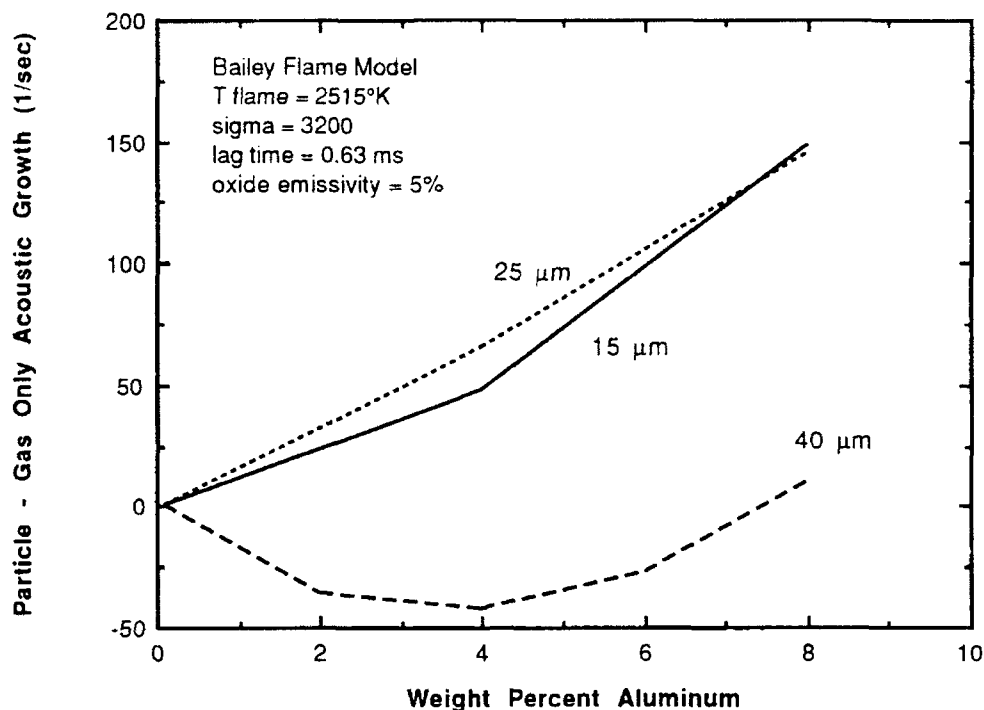
Figure 8.2 Acoustic growth rate versus percent aluminum for the revised Bailey model using various sizes of aluminum.

This result can be explained as follows. The acoustic mode shape and location of nodes and antinodes of the standing wave is determined by the temperature profile within the burner. If the temperature profile is changed, then the location of the acoustic nodes and antinodes in the burner is also changed. Maximum driving occurs when the velocity antinode is located at the Rijke burner flame. Changes in the temperature profile due to aluminum combustion can move the velocity antinode towards the flame, resulting in an increase in acoustic growth or away from the flame, resulting in a decreased acoustic growth. For all of the conditions and Rijke flame models studied, this "indirect" mechanism of distributed combustion can be a significant portion of the acoustic growth (e.g. 30 to 100% of the increase due to the aluminum particles).

Key particle parameters effecting this aspect of distributed combustion include the percent aluminum and the emissivity of the smoke created. Particle diameter and oxidizer concentration have a somewhat of lesser effect. Ignition delay temperature has very little effect on the acoustic growth change due to a mode shift. Oxide emissivity has the largest effect on the acoustic growth (See Figure 8.3). Although the emissivity of a single particle of oxide is quite well quantified (e.g. 0.47 at 1500°K), the effective emissivity in a cloud of oxide particles is more difficult to determine. Raun used a value of 0.25 for the emissivity of the oxide. Glassman (1992), on the other hand, suggests that in a cloud of particles, there are little radiative heat losses because a single particle sees primarily particles of the same temperature. A reasonable emissivity value for a cloud may well be very small. Because of its importance in defining the temperature profile, further research is needed in this area.

31
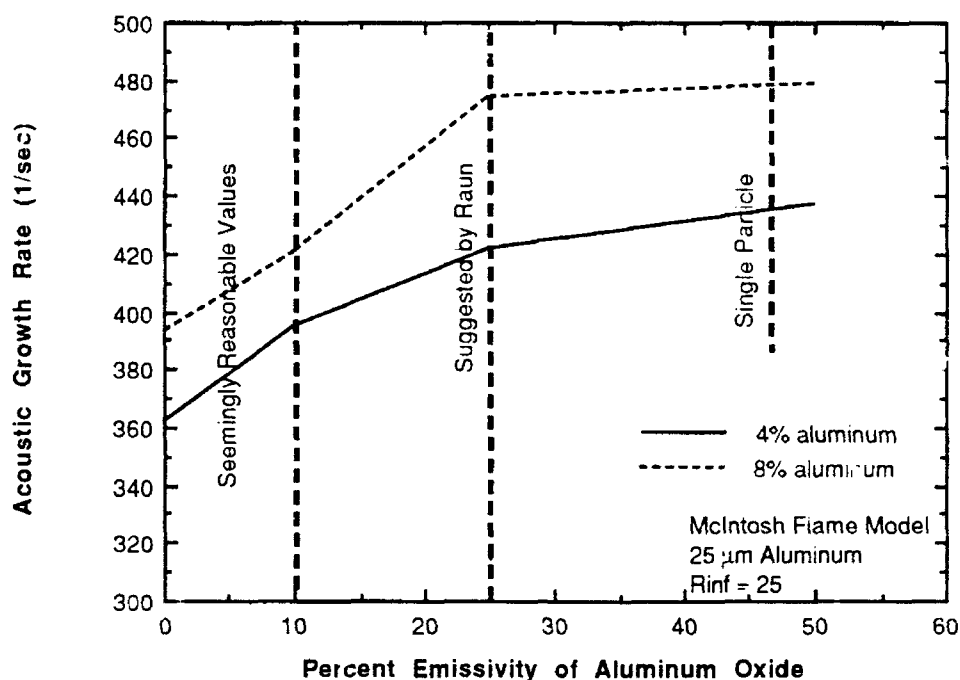
Figure 8.3 Rijke acoustic model calculated acoustic growth rate as a function of aluminum oxide emissivity. Increased emissivity causes a drop in hot section temperature profile.

As evidence of the indirect mechanism of distributed combustion, Barron (1991) noted an increase in acoustic growth in the Rijke burner with the addition of aluminum oxide particles. This increase was originally attributed to some possible catalytic effect. Because aluminum oxide does not burn, the direct distributed combustion effects due to fluctuating reaction rate would not be present. It would not seem unreasonable, however, that the introduction of the aluminum oxide would cool the hot section of the burner sufficiently either due to heat absorbed or radiated to cause a shift in the mode such that the acoustic velocity antinode was nearer the flame. This would result in the increased acoustic growth seen experimentally.

In addition to changes in the acoustic growth due to a mode shift, the Rijke burner flame model increases the magnitude of the acoustic properties in the hot section of the tube. Such increases yield increased values of the fluctuating reaction rates as Equation 8.2 would suggest. Therefore, the acoustic growth due to the fluctuating reaction and flame couple to effect a much larger value than their individual components. Such a result is illustrated in Figure 8.4.

8.2.4 Relaxation of the Assumptions in Perturbation Theory

Two difficulties are encountered when using simple perturbation theory to solve for the fluctuating particle reaction rate, rather than solving the unsteady conservation equations in their entirety. The first difficulty is that of taking derivatives of empirical correlations. The majority of the aluminum combustion model is based on conservation equations. Taking derivatives of these equations should be possible without losing the physical nature of the solution. In contrast, calculation of the derivative of the reaction rate with respect to velocity requires the use of a Nusselt

32

number correlation. Unlike continuity equations, the Nusselt number correlation is created by fitting experimental data. The functional form of the correlation may not be physically correct. Therefore, when the derivative is taken, it may not represent physical reality. Error from perturbing such empirical correlations is difficult to determine but may be significant.
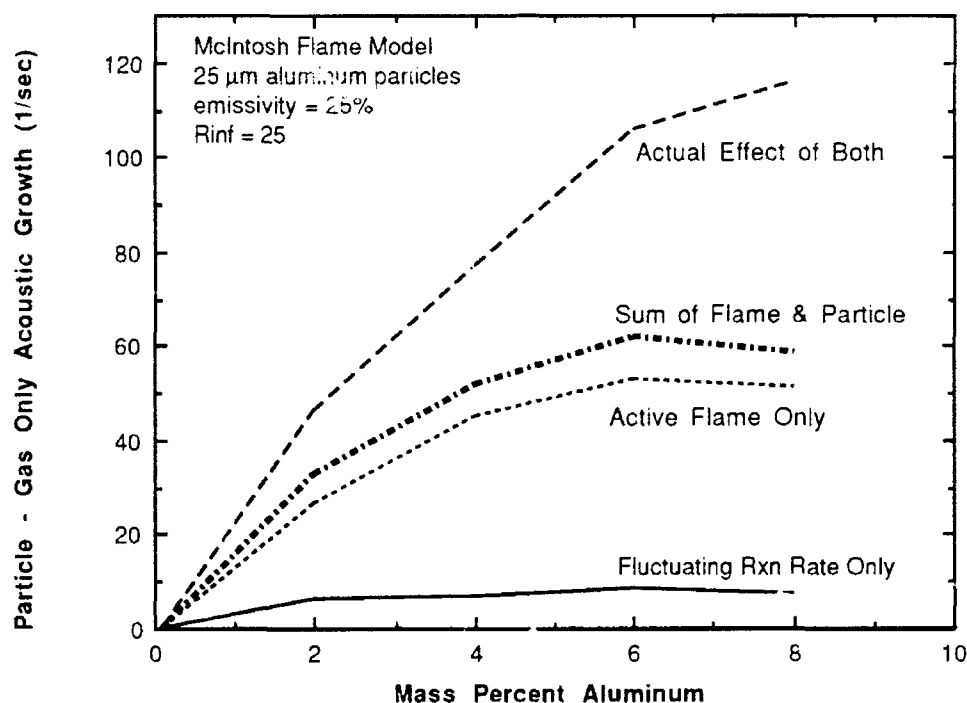
Figure 8.4 Increase in acoustic growth due to addition of aluminum with and without fluctuating reaction rate and acoustically active flame. Note sharp increase with combined effects as compared to sum of individual effects.

The second difficulty associated with perturbation theory is that this approach assumes that the reaction rate responds instantaneously to the acoustic properties. For a diffusion-limited process, it would seem that changes in the bulk of the fluid would not have an instantaneous effect on the fluctuating reaction rate or heat release, but that there would be a lag time associated with the aluminum combustion.

Further evidence of the need for a lag time can be seen in the results of using the Bailey flame response to model the propane flame in the Rijke burner. The Bailey model uses two parameters to fit experimental data: a flame ignition delay time and the derivative of the flame speed with respect to the flame holder. To obtain the acoustic growth rates due to burning aluminum shown in Figure 8.2, the flame ignition delay time in the Bailey model would have to be on the order of milliseconds. In contrast, measured propane flame time lags are on the order of microseconds. A time lag of milliseconds is actually more characteristic of particle combustion, than a premixed flame. Thus, the Bailey flame model can produce results similar to experiment by simulating the time lag associated with burning particles. Although

strictly an artifact of the mathematical model. such a result does suggest the need for a time lag in the aluminum combustion model as suggested previously by Raun.

In an effort to acccunt for such a lag, the fluctuating reaction model was modified to include a delay time of the form:

$$\hat{r}_p = \left(\frac{\partial r_p}{\partial T_g} \hat{T}_g + \frac{\partial r_p}{\partial p} \hat{p} + \frac{\partial r_p}{\partial \rho_p} \hat{\rho}_p + \frac{\partial r_p}{\partial v_g} \hat{v}_g \right) e^{-i\omega \tau}$$

(8.6)

where ω_0 is the frequency of oscillation and τ is the lag time. This time lag is based on the time required for the oxidizing species and temperature effects in the bulk to be felt at the flame surrounding the aluminum particle. Its value is calculated from the steady-state aluminum combustion model. The problem becomes one of determining the thickness of the region through which changes in acoustic properties must travel to influence conditions at the aluminum diffusion flame (r_{inf}). The thickness of this region could be as great as the interparticle distance. Calculated values of the interparticle distance vary from ~40 diameters at fifteen percent particles to ~80 diameters at two percent. The actual location of the boundary layer (or r_{inf}) is believed to be somewhere between the flame front and this interparticle separation distance.

Values of r_{inf} in the range of 10 to 35 particle diameters were investigated (See Figure 8.5), and compare favorably to the calculated value of 20 determined by Mussarra, et. al. (1986) for a coal particle in Stokes flow. At a value of 25, there exists a maximum acoustic growth. Not surprisingly, this maximum corresponds to a 90° phase shift. With this phase shift, the energy release due to a velocity perturbation would be in phase with the pressure as predicted by the Rayleigh criteria.
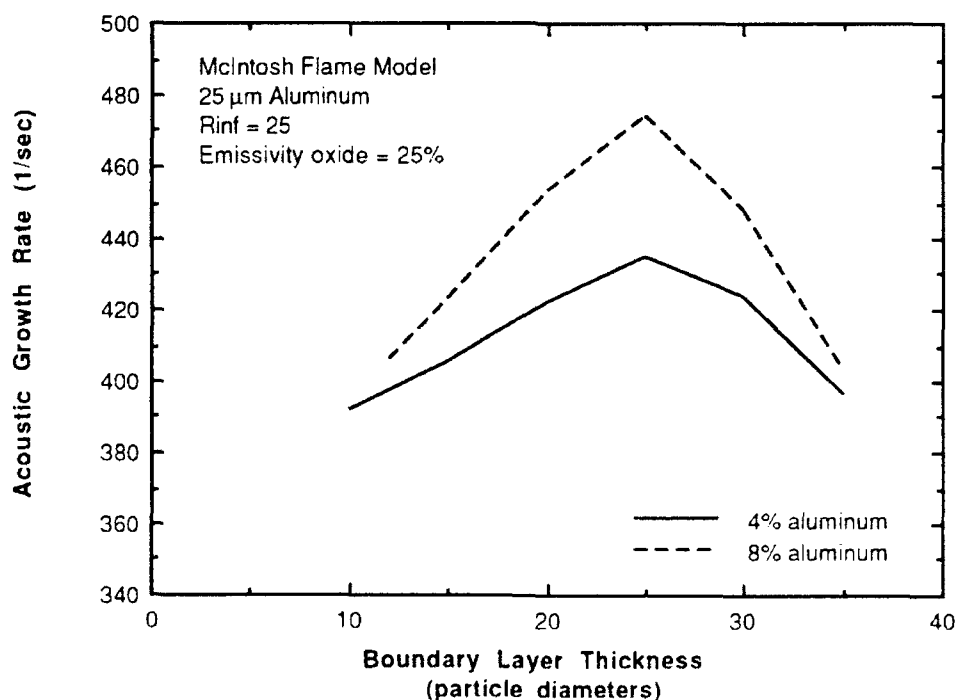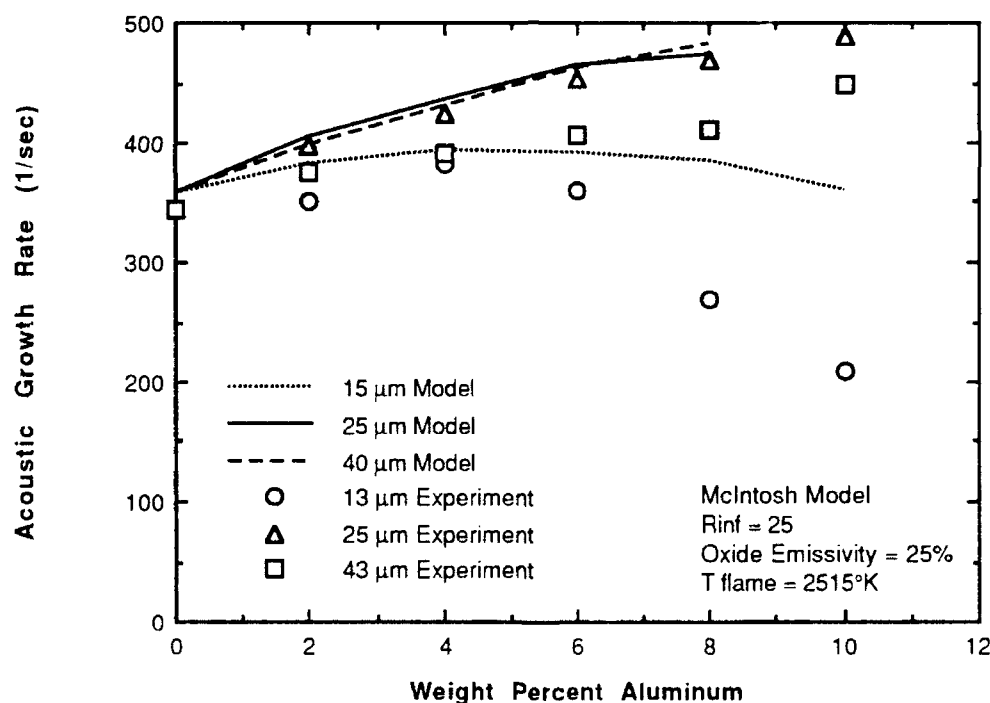

Figure 8.5 Acoustic growth as a function of the region of influence or r_{inf}

As mentioned previously, the fluctuating reaction rate without the time lag was an order of magnitude too small. By including the lag, the acoustic velocity component of the reaction rate becomes dominant over the acoustic pressure component. The importance of the acoustic velocity in the calculation of the fluctuating reaction rate was proposed by Beckstead and Brooks (1990) and Rundinger (1975).

8.2.5 Comparison with Experimental Work

Using an r_{inf} value of 25 and an emissivity value of 0.25, the Rijke acoustic model was compared to the work of Barron (See Figure 8.6). The values predicted by the new Rijke model compare reasonably well with the experimental data at low concentration. The order of magnitude of the acoustic growth rate is correct, and there is an increase in acoustic growth for larger fluxes of aluminum particles. At higher aluminum concentrations, however, the model and experiment are more dissimilar. Reasons for such variations can stem from either the model or experimental data.

Figure 8.6 Acoustic growth as a function of weight percent aluminum for the Rijke acoustic model and the experimental work of Barron (1991).

Certain aspects of the experimental data remain in question. As mentioned previously, a constant flow particle feeder has been difficult to obtain especially for small particle sizes. It has been suggested that the drop in acoustic growth for the 15 μm aluminum particles could be the result of inconsistencies in the particle feeder. At high aluminum mass fluxes, such errors are magnified, resulting in the larger data

35

scatter at high concentrations. In addition, the particles used experimentally are not a single diameter, but rather a wide size distribution, resulting in varying burn rates and heat transfer characteristics. Efforts are currently underway to obtain improved experimental data and resolve the particle feeder and size distribution difficulties.

The model assumes that the particles burn as individuals, not affected by those surrounding them. It is believed that at concentrations greater than 8% aluminum, group combustion is probably occurring as evidenced by the photographs taken in the work by Barron (1991). Individual particles cannot be seen; a bright ball of fire exists in the reaction zone. Under these conditions, the combustion mechanism is different and the assumptions of the mean and oscillatory aluminum reaction models break down. According to the study of group theory by Chiu (taken from Kuo, 1986), even 1% aluminum would result in group combustion for the particles in question. However, Chiu assumes that the oxidizer must diffuse from the surroundings into the cloud for combustion to occur. In the case of the Rijke burner, the particles are premixed with the oxidizer, thus the equations of Chiu would have to be rederived for this situation.

9.0 CONCLUSIONS AND RECOMMENDATIONS

Since a primary purpose of this work is to improve the mathematical model of the Rijke burner previously developed by Raun (1984), this section is divided according to the primary thrusts of improvement: (1) the McIntosh flame response model, (2) the aluminum combustion model, and (3) the Rijke program including the McIntosh flame response and aluminum combustion.

9.1 The McIntosh Flame Response

To understand the interaction between the propane flame and acoustics in the Rijke burner, the McIntosh flame model was included into the Raun Rijke program. Because of its more fundamental nature, this transfer function describes the physics of the Rijke burner better than with previous phenomenological approaches. In addition, the model requires relatively few unknowns and is based on reasonable assumptions for study in the Rijke burner.

Analysis of the propane flame model indicates that small changes in properties such as flame temperature can result in large changes in acoustic growth rate. If this flame model is an accurate representation of the Rijke burner, these "resonant" type properties would explain the difficulty of obtaining reproducible data.

By adjusting the flame temperature or the flame holder impedance, the experimental work of Finlinson (1988) was fit within 10% for both frequency and acoustic growth rate. In addition, the model was able to predict the complex mode shifts seen experimentally.

In addition to the factors previously included in the Law derivation, the model of this study was expanded to include the effects of multiple oxidizers and their products, oxide accumulation on the surface of the burning aluminum particle, and convection. There are no adjustable parameters in the improved aluminum combustion model, and both transport and thermodynamic properties are calculated internally.

Results indicated that simple empirical models, based on a summed mole fraction of oxidizer, could be erroneous in environments which contain oxygen, water and carbon dioxide. The aluminum combustion model was compared to experimental data from burners, laser-ignited particles, and propellant under a variety of conditions. In spite of large data scatter, the aluminum combustion model compares more favorably to experimental data than the simple liquid droplet model. The discrepancy in the comparison between the model and experimental data is believed to be due both to difficulties in obtaining experimental data and shortcomings of the model due to the complexity of aluminum combustion.

9.3 The Rijke Burner Model

The McIntosh flame model and the aluminum combustion model were implemented into the Rijke program, and the mean and acoustic properties of the burner were studied separately.

Efforts to characterize the location and amount of heat transfer between phases yielded the following: (1) Comparison with experimental work suggests an ignition temperature of ~1900 K for conditions found in the Rijke burner. (2) The size of the aluminum particle, the concentration of the aluminum and its oxidizer, and the emissivity of the metal oxide are important to proper gas temperature profile determination.

By carrying out linear perturbation of the time-mean aluminum combustion model, the effects of aluminum combustion on the acoustics in the burner were determined. Similar to the results of Raun, the increase in acoustic growth due to the addition of aluminum was a factor of ten lower than corresponding experimental data. Using the more complex model of aluminum combustion did not appear sufficient to cause the proper increase in acoustic growth. The flame/acoustic interaction and the fluctuating reaction rate were studied to improve the fit of the experimental data.

Calculations have shown that a significant part of the acoustic growth with the addition of aluminum was due strictly to the change in the gas temperature profile. The change in temperature profile could cause the location of the velocity antinode to shift relative to the Rijke burner flame and thereby cause an increase in the flame response. The flame response can also couple with the fluctuating particle reaction rate resulting in a synergistic increase in acoustic growth over the individual effects.

To further improve the fluctuating aluminum combustion model, a time lag between the acoustic properties and the fluctuating heat release was added. This time lag is based on the length of time needed for an effect in the bulk to be transmitted to the aluminum diffusion flame through the boundary layer. For a boundary layer thickness of approximately 25 particle diameters, the time lag shifted the effects of the acoustic velocity 90° out of phase. Such a boundary layer thickness is very reasonable, and results in the heat release being in phase with the acoustic pressure. At this condition, maximum acoustic driving occurs.

The new Rijke acoustic model agreed within 5% of the acoustic growth rates observed by Barron for 25 μm aluminum particles. Discrepancies between experiment

The new Rijke acoustic model agreed within 5% of the acoustic growth rates observed by Barron for 25 μm aluminum particles. Discrepancies between experiment and model for the 13 and 43 μm aluminum particles were larger, but similar qualitative trends were seen.

9.4 Recommendations for Future Work

9.4.1 The McIntosh Flame Response
Because the flame response is such an important driving factor in the Rijke burner, further study is warranted. The McIntosh model assumes that the thermal conductivity is linearly proportional to the temperature. While this assumption is reasonable over a limited range of temperatures, the extrapolation of thermal conductivity to temperatures at the burner flame can result in serious error in the calculation of the thermal conductivity. Making the thermal conductivity a more complex function of temperature should make the model more realistic.

Experimental efforts should focus on measuring the flame temperature and temperature profile. These parameters are essential to determining *a priori* what the acoustic growth will be.

9.4.2 Aluminum Combustion Model
A more complex approach could be taken to better describe aluminum combustion. Such an effort would most likely require a numerical rather than analytical solution. This model would not necessarily be used in the Rijke program. but would assist in understanding the complex process of aluminum combustion. A numerical model should include equilibrium calculations of aluminum reaction, since it is not an irreversible reaction as assumed in the current model. Variable transport properties would also need to be included, as they have been found to be important.

Once again, better experimental data is needed to aid in understanding aluminum combustion. More carefully controlled and quantified environmental conditions are necessary to properly compare experimental data to the model. High pressure aluminum combustion without the distorting effects of propellant should also be obtained.

9.4.3 Rijke Burner Model
The heat transfer in the hot section should be better characterized experimentally. Radiative heat transfer from the metal oxide and heat loss to the surroundings must be better quantified. An understanding of the effects of modeling a two-dimensional temperature distribution with a one-dimensional plug flow model must be better understood. both in the mean and acoustic portions of the Rijke acoustic model.

Future research should include calculation of a time lag between the acoustic properties and the particle responses. Solution of the full transient conservation equations for particle reaction may be necessary to describe such an interaction. Time lag often creates numerical instabilities in the program. Therefore, it may be necessary to use a more stable numerical approach.

10.0 REFERENCES

Bailey, J. J., "A Type of Flame-Excited Oscillation in a Tube", Journal of Applied Mechanics, September 1957, Vol. 24, No. 3, pp. 333-339.

Barron, James T., "An Experimental Study on the Effects of Dispersed Particles on Acoustic Growth Rates in a Modified Rijke Burner," M. S. Thesis, Brigham Young University, August 1991.

Bartlett, R. W., Ong, J. N. Jr., Fassell, W. M. Jr. and Papp, C. A., "Estimating Aluminum Particle Combustion Kinetics," Combustion and Flame, September 1963, Vol. 7, pp. 227-234.

Bayly, B. J., "Onset and Equilibrium of Oscillations in General Rijke Devices," Journal of the Acoustical Society of America, March 1986, Vol. 79, No. 3, pp. 846-850.

Beckstead, M. W. and Brooks K. P., "A Model for Distributed Combustion in Solid Propellants." 27th JANNAF Combustion Meeting, 1990, Vol. II, pp. 237-258.

Beckstead, M. W., "Evidences for Distributed Combustion," 24th JANNAF Combustion Meeting, 1987, Vol. I, pp. 1-12.

Beckstead, M. W. , Braithwaite, P.C., and Gordon, D. L. "Measurements of Distributed Combustion", 1985, AGARD -CP-391, Smokeless Propellants, pp.21-1.

Beckstead, M. W. , Richards, R.S., and Brewster, B.S. "Distributed Combustion Effects of Particle Damping", AIAA J., 1984, 22, 3, pp.383-387.

Beckstead, M. W. "Distributed Combustion: A Mechanism of Acoustic Suppression", 21st JANNAF Combustion Meeting, 1984, Vol I, CPIA No 412, pp.187-194.

Bird, R. B., Stewart, W. E., and Lightfoot, E. N., Transport Phenomena, John Wiley and Sons, Inc., New York, NY, (1960).

Blomshield, F. S. , Kraeutle, K.J., Stalnaker, R.A., Beckstead, M.W., and Stokes, B. "Aluminum Combustion Effects of Combustion Instability of High Burn Rate Propellants", 28th JANNAF Combustion Meeting, 1991, Vol. III, CPIA No. 573, pp.419-438.

Bosscha, H. and Riesse, P., Pogg. Ann., 1859, Vol 108, pp. 653.

Braithwaite, P. C., "Measurements of Distributed Combustion in the Rijke Burner," M.S. Thesis, Brigham Young University, December 1984.

Braithwaite, P. C. , Beckstead, M.W., and Raun, R.L. "Measurements of Distributed Combustion", 21st JANNAF Combustion Meeting, 1984, Vol I, CPIA No 412, pp.177-186.

Brzustowski, Thomas A. and Glassman, Irvin, "Spectroscopic Investigation of Metal Combustion," <u>Progress in Astronautics and Aeronautics</u>, 1964a, Vol. 15: Heterogeneous Combustion, pp. 41-73.

Brzustowski, Thomas A. and Glassman, Irvin, "Vapor-Phase Diffusion Flames in the Combustion of Magnesium and Aluminum I. Analytical Developments," <u>Progress in Astronautics and Aeronautics</u>, 1964b, Vol. 15: Heterogeneous Combustion, pp. 75-115.

Carrier, G. F., "The Mechanics of the Rijke Tube," <u>Quarterly of Applied Mathematics</u>, April 1954, Vol. XII, No. 1, pp. 383-395.

Carrier, George F., Fendell, Francis E., and Bush, William B., "Stoichiometry and Flameholder Effects on a One-Dimensional Flame," <u>Combustion Science and Technology</u>, 1978, Vol. 18, pp. 33-46.

Carvalho, J. A. Jr., Ferreira, M. A., Bressan, C., and Ferreira, J. L. G., "Definition of Heater Location to Drive Maximum Amplitude Acoustic Oscillations in a Rijke Tube," <u>Combustion and Flame</u>, 1987.

Charagundia, S. Rao and Pellett, G. L., "Transient Processes in Metal Droplet Combustion," <u>19th JANNAF Combustion Meeting</u>, 1982, Vol. 1, pp. 41-52.

Chung, S. H., and Law, C. K., "Importance of Dissociation Equilibrium and Variable Transport Properties on Estimation of Flame Temperature and Droplet Burning Rate," <u>Combustion and Flame</u>, 1984, Vol. 55, pp. 225-235.

Clarke, J. F. and McIntosh A. C., "The Influence of a Flameholder on a Plane Flame Including Its Static Stability," <u>Proceedings of the Royal Society of London</u>, Series A, 1980, Vol. 372, pp. 367-392.

Crump, J. E., Prentice, J. L., and Kraeutle, K. J., "Role of Scanning Electron Microscope in the Study of Solid Propellant Combustion: II. Behavior of Metal Additives." <u>Combustion Science Technology</u>, 1969, Vol. 1, pp. 205-223.

Culick, F. E. C. "Formulation of an Example Showing the Possible Influence of Residual Burning on Particle Damping in a T-Burner", Jan. 2, 1975, memo to M.W. Beckstead, Hercules, Inc.

Culick, F. E. C. "Influence of Residual Combustion", Sept. 26 1974, memo to M.W. Beckstead, Hercules, Inc.

Davis, A., Solid Propellants: "The Combustion of Particles of Metal Ingredients," <u>Combustion and Flame</u>, December 1963, Vol. 7, pp. 359-367.

Diederichsen, J., "A Singing Flame as a tool for Evaluation of Damping Agents for Solid Propellant Rocket Motors," <u>Combustion and Flame</u>, March 1963, Vol. VII, No. 1, pp. 30-37.

Ermakov, V. A., Razdobreev, A. A., Skorik, A. I., Pozdeev, V. V., and Smolyakov, S. S., "Temperature of Aluminum Particles at the Time of Ignition and Combustion," Translated from: Fizika Goreniya i Vzryva, 1982, Vol. 18, No. 2, pp. 141-143.

Finlinson, Jerry Curt, "Experimental Characterization of a Modified Rijke Burner," M. S. Thesis, Brigham Young University, August 1988.

Finlinson, J. C. , Nelson, M.A., and Beckstead, M.W. "Characterization of a Modified Rijke Burner for Measurement of Distributed Combustion", 24th JANNAF Combustion Meeting, 1987, Vol I, CPIA No 476, pp.13-26.

Fontijn, Arthur and Futerko, Peter M., "Homogeneous Kinetics of Metal Species Over Wide Temperature Ranges: Techniques, Measurements, and Correlations," (Prepared for Publication in Gas-Phase Metal Reactions).

Frank-Kamenetski, D. A., Diffusion and Heat Transfer in Chemical Kinetics, Plenum, 1969.

Friedman, R. and Macek, A., "Combustion Studies of Single Aluminum Particles," Ninth Symposium (International) on Combustion, 1963, 703-712, Academic Press, New York.

Friedman, R. and Macek, A., "Ignition and Combustion of Aluminum Particles in Hot Ambient Gases," Combustion and Flame, March 1962, Vol. 6, pp. 9-19.

Garris, C. A., Toong, T.-Y., and Patureau, J.-P., "Chemi-Acoustic Instability Structure in Irreversibly Reacting Systems," ACTA Astronautica, November-December 1975, Vol. 2, Nos. 11-12, pp. 982-997.

Glassman, I., Papas, P., and Brezinsky, K., "A New Definition and Theory of Metal Pyrophoricity," Combustion Science and Technology, 1992, Vol. 83, pp. 161-165.

Glassman, Irvin, Combustion, New York, Academic Press, 1977.

Gremyachkin, V. M., Istratov, A. G., and Leipunskii O. I., "Effect of Immersion in a Flow on Metal-Drop Combustion," Combustion, Explosion, & Shock Waves, 1979, Vol. 15, No. 1, pp. 26-29.

Gremyachkin, V. M., Istratov, A. G., and Leipunskii, O. I., "Model for the Combustion of Metal Droplets," Combustion, Explosion, & Shock Waves, 1975, Vol. 11, No. 3, pp. 313-318.

Hartman, K. O., "Ignition and Combustion of Aluminum Particles in Propellant Flame Gases," 8th JANNAF Combustion Meeting, November 1971, Vol. 1, CPIA #220, pp. 1-24.

Hunter, Hugh W., "Aluminum Particle Combustion Progress Report," NOTS TP 3916, April 1964 - June 1965.

Joos, F. and Vortmeyer, D., "Self-Excited Oscillations in Combustion Chambers With Premixed Flames and Several Frequencies," Combustion and Flame, 1986, Vol. 65, pp. 253-262.

Joulin, G. and Mitani, T., "Linear Stability Analysis of Two-Reactant Flames," Combustion and Flame, 1981, Vol. 40, pp. 235-246.

Kaskan, W. E., "An Investigation of Vibrating Flames," 4th Symposium (International) on Combustion, 1953, Vol. 4, pp. 575-591.

Katto, Yoshiro and Sajiki, Akira, "Onset of Oscillation of a Gas-Column in a Tube Due to the Existence of Heat-Conduction Field (A Problem of Generating Mechanical Energy From Heat)," Bulletin of the JSME, September 1977, Vol. 20, No. 147, pp. 1161-1168.

King, Merrill K., "Modeling of Single Particle Aluminum Combustion in CO_2-N_2 Atmospheres," 17th Symposium (International) on Combustion, 1977, pp. 1317-1328.

Kudryavtsev, V. M., Sukhov, A. V., Voronetskii, A. V., and Shpara, A. P., "High Pressure Combustion of Metals (Three-Zone Model)," Combustion, Explosion, & Shock Waves, 1979, Vol. 15, No. 6, pp. 731-737.

Kuehl, Donald, "Ignition and Combustion of Aluminum and Beryllium," AIAA Journal, 1965, Vol. 3, No. 12, pp. 2239.

Kuo, Kenneth Kuan-yun, Principles of Combustion, New York, John Wiley & Sons, 1986.

Law, C. K. and Williams, F. A., "On a Class of Models for Droplet Combustion," AAIA Paper No. 74-147, 1974.

Law, C. K., "A Simplified Theoretical Model for the Vapor-Phase Combustion of Metal Particles," Combustion Science and Technology, 1973, Vol. 7, pp. 197-212.

Macek, Andrej, "Fundamentals of Combustion of Single Aluminum and Beryllium Particles," Eleventh Symposium (International) on Combustion, 1967, pp. 203-2143.

Mann, D. M., "Particulate Formation in Aluminum/Oxygen Flames," 15th JANNAF Combustion Meeting, September 1978, Vol. II, pp. 337-347.

Mawardi, O. K., "Aero-Thermoacoustics (The Generation of Sound by Turbulence and by Heat Sources)," Reports on Progress in Physics, 1956, Vol. XIX, pp. 156-187.

McIntosh, A. C. and Clarke, J. F., "Resonant Response of a Flat Flame Near a Flame Holder," Progress in Astronautics and Aeronautics, 1981, Vol. 88: Flames, Lasers, and Reactive Systems, pp. 3-37.

McIntosh, A. C., "Combustion-Acoustic Interaction of a Flat Flame Burner System Enclosed Within an Open Tube," Combustion Science and Technology, 1987. Vol. 54, pp. 217-236.

McIntosh, A. C., "Short Communication On Flame Resonance in Tubes," Combustion Science and Technology, 1990, Vol. 69, pp. 147-152.

McIntosh, A. C., "The Effect of Upstream Acoustic Forcing and Feedback on the Stability and Resonance Behavior of Anchored Flames," Combustion Science and Technology, 1986, Vol. 49, pp. 143-167.

Merk, H. J., "Analysis of Heat-Driven Oscillations of Gas Flows: III. Characteristic Equation for Flame-Driven Oscillations of the Organ-Pipe Type," Applied Scientific Research, 1957-58a, Vol. A7, p. 175, (as referenced by Putnam, 1964a).

Micheli, Paul L. and Schmidt, Wilfred G., "Behavior of Aluminum in Solid Rocket Motors," January 1977, AFRPL-TR-76-58.

Musarra, S. P., Fletcher, T. H., Niksa, S. and Dwyer, H. A., "Heat and Mass Transfer in the Vicinity of a Devolatilizing Coal Particle," Combustion Science and Technology, 1986. Vol. 45, pp. 289-307.

Pokhil, P. F., Belyayev, A. F., Frolov, Yu. V., Logachev. V. S., and Korotkov, A. I., "Combustion of Powdered Metals in Active Media," October 18, 1973, FTD-MT-24-551-73.

Prentice, Jack L., "Aluminum Droplet Combustion: Rates and Mechanisms in Wet and Dry Oxidizers," NWC TP 5569, April 1974.

Price, E. W., "Combustion of Metallized Propellants," Progress in Astronautics and Aeronautics, 1984b, Vol. 90: Fundamentals of Solid-Propellant Combustion, pp. 479-513.

Price, E. W., "Experimental Observations of Combustion Instability," Progress in Astronautics and Aeronautics, 1984a, Vol. 90: Fundamentals of Solid-Propellant Combustion., 733-790.

Price, E.W., Kraeutle, K.J., Prentice, J.L., Boggs, T.L., Crump, J.E., and Zurn, D.E., "Behavior of Aluminum in Solid Propellant Combustion," NWC TP 6120, March 1982.

Raun, R.L., Beckstead, M.W., Finlinson, J.C., and Brooks, K.P., "A Review of Rijke Tubes, Rijke Burners and Related Devices", accepted for publication in Progress in Combustion and Energy Science, 1993.

Raun, R. L. and Beckstead, M.W. "A Numerical Model for the Rijke Burner", 22nd JANNAF Combustion Meeting, 1985, Vol I. CPIA No 432, pp.123-132.

Raun, R. L. and Beckstead, M.W. "A Numerical Model for Temperature Gradient and Particle Effects on Rijke Burner Oscillations", accepted for publication in Combustion and Flame, 1993.

Raun, R. L., "A Numerical Model for the Rijke Burner," PhD. Dissertation, Brigham Young University, December 1985.

Rayleigh, J. W. S., "The Explanation of Certain Acoustical Phenomena," Nature, 1878, Vol. 18, pp. 319-321.

Razdobreev, A. A., Skorik, A. I., and Frolov, Yu. V., "Ignition and Combustion Mechanism in Aluminum Particles," Combustion, Explosion, & Shock Waves, 1976.

Richardson, "The Singing Flame," Proceedings of the Physical Society of London, Vol. 35, p. 47.

Rijke, P. L., "Notice of a New Method of Causing a Vibration of the Air Contained in a Tube Open at Both Ends," Philosophical Magazine, 1859, Vol. 17, pp. 419-422.

Rogowski, Donald F., English, Andrew J. and Fontijn, Arthur. "A High-Temperature Fast-Flow-Reactor Kinetics Study of the Reaction $AlO + CO_2 \rightarrow AlO_2 + CO$. Thermochemical Implications," Journal of Physical Chemistry, 1986, Vol. 90, pp. 1688-1691.

Rundinger, G., "Effect of Velocity Slip on the Burning Rate of Fuel Particles," Journal of Fluids Engineering, September, 1975, pp. 321-326.

Schimmer, H. and Vortmeyer, D., "Acoustical Oscillation in a Combustion System with a Flat Flame," Combustion and Flame, 1977, Vol. 28, pp. 17-24.

Shah, R. K. and London, A. L., Laminar Flow Forced Convection in Ducts, Academic Press, New York, 1978.

Stone, W. C. "Workshop report - Acoustic Instability in a High Burning Rate - High Pressure Propellant", 21st JANNAF Combustion Meeting, 1984, Vol II, CPIA No 412, pp.113-118.

Wheatley, John, Hofler, T., Swift, G. W., and Migliori, A., "Understanding some Simple Phenomena in Theromoacoustics with Applications to Acoustical Heat Engines," American Journal of Physics, February 1985. Vol. 53, No. 2.

Wilson, R. P. Jr. and Williams. F. A., "Experimental Study of the Combustion of Single Aluminum Particles in O_2/Ar.," Thirteenth Symposium (International) on Combustion, 1971, pp. 833-845.

APPENDIX A - Flame Transfer Function Equations

McIntosh Flame Transfer Function

The McIntosh flame transfer function will now be briefly described. The conservation equations used in its derivation include the continuity, energy, species, and momentum equations, respectively:

$$\frac{\partial \rho}{\partial t} + \frac{\partial}{\partial x}(\rho u) = 0 \tag{A.1}$$

$$\frac{\partial T}{\partial t} + u\frac{\partial T}{\partial x} - \frac{1}{Le\ \rho}\frac{\partial}{\partial x}\left(\lambda\frac{\partial T}{\partial x}\right) = Le(1+\sigma)Q_1\Lambda_1 C_l(C_l+|\Delta_1|)\ exp[\theta_1(1-1/T)]$$

$$+ \frac{T_{0_1}(1-\gamma^1)}{\rho}\left[\frac{\partial p}{\partial t} + u\frac{\partial p}{\partial x} + \frac{4}{3}\gamma M^2\ Sc\ \lambda\left(\frac{\partial u}{\partial x}\right)^2\right] \tag{A.2}$$

$$\frac{\partial C_l}{\partial t} + u\frac{\partial C_l}{\partial x} - \frac{1}{\rho}\frac{\partial}{\partial x}\left(l\frac{\partial C_l}{\partial x}\right) = - Le\ \Lambda_1 C_l(C_l+|\Delta_1|)\ exp[\theta_1(1-1/T)] \tag{A.3}$$

$$\frac{\partial u}{\partial t} + u\frac{\partial u}{\partial x} + \frac{1}{\gamma M^2\rho}\frac{\partial p}{\partial x} = \frac{4}{3}\frac{Sc}{\rho}\frac{\partial}{\partial x}\left(\lambda\frac{\partial u}{\partial x}\right) \tag{A.4}$$

The following is a list of some of the key assumptions in the McIntosh derivation.

- One-dimensional
- $t_{acoustic} \sim t_{diffusion}$
- $\lambda * \rho$ is constant
- Lewis number not restricted to one

- Mach number << 1
- Ideal gas law
- Infinite flame holder conductance
- Thin flame zone

Using these assumptions, an expression relating acoustic velocity upstream of the flame ($\bar{u}_{u0}$) and the acoustic velocity downstream of the flame ($\bar{u}_{u\infty}$) can be written as:

$$\bar{u}_{u\infty} = - \frac{\bar{u}_{u0}V}{T_{01}} \tag{A.5}$$

where T_{01} is the ratio of temperatures before and after the flame. The transfer function V is given by the expression:

$$V = \frac{-\omega B}{Le\ G\left(\frac{1}{2} - s\right)} - T_{01} - \frac{A}{G}X_1 + \frac{Le\ B_1}{\omega}(X_1 - X_2 e^{-Lex_{in}}) \tag{A.6}$$

where Le_c is the Lewis number and x_{1f1} is the dimensionless flame standoff distance. The symbol ω is a complex dimensionless frequency defined by the equation:

$$\omega = i\omega' \frac{D'}{v'^2} \tag{A.7}$$

where ω is the dimensional frequency and D' and v' are the dimensional diffusivity and velocity at inlet conditions. In addition the following terms used in the calculation of V are defined below:

$$X_{2,1} = \frac{1}{2} \pm S \pm \frac{s \, e^{\pm 1/2 \, Le \, x_{in}}}{\sinh(Le \, s \, x_{in})} \qquad\qquad A = \frac{Le \, B_1}{\omega\left(\frac{1}{2} - S\right)} X_1\left(G - \frac{\omega}{Le}\right) + B_1 Y$$

$$B = \frac{2}{\theta_1}\left[X_1 - \left(\frac{1}{2} - S\right)Y\right] \qquad\qquad Y = 1 + \frac{r \, e^{-1/2 \, x_{in}}}{\sinh(r \, x_{1f1})}$$

$$G = D + \frac{2}{\theta_1 B_1}\left[\left(\frac{1}{2} + R\right)(s + S) + D\right]\left(\frac{1}{2} - S\right) \qquad D = s^2 - \frac{1}{2}S + \frac{1}{2}R - RS$$

$$R = r \coth(r \, x_{1f1}), \quad S = s \coth(Le \, s \, x_{1f1}) \qquad\qquad r = \sqrt{\omega + \frac{1}{4}}, \quad s = \sqrt{\frac{\omega}{Le} + \frac{1}{4}}$$

$$B_1 = \frac{1 - T_{01}}{1 - e^{-Le \, x_{in}}} \tag{A.8-A.16}$$

Impedance of the flame holder was described as:

$$\frac{|p'|_{x=0^+} - |p'|_{x=0^-}}{|u'|_{burner}} = \gamma Z \tag{A.17}$$

where p' is the acoustic pressure before and after the burner, u' is the acoustic velocity at the burner and Z and γ are the acoustic impedance and ratio of specific heats.

Joulin and Mitani Critical Lewis Number

The calculation of the Lewis number for the propane flame was based on the work of Joulin and Mitani (1981) from the equation:

$$Le_c = Le_l + J\,(Le_r - Le_l) \tag{A.18}$$

were Le_c, Le_l, and Le_r are the calculated critical Lewis number, the lean species Lewis number and the rich species Lewis number, respectively. The value of J can be calculated from

$$J = n \frac{G(m, n-1, A)}{G(m, n, A)} \tag{A.19}$$

$$G(m,n,A) = \int_0^\cdot \xi^m(\xi+A)^n e^{-\xi}\, d\xi$$

<div align="right">(A.20)</div>

$$A = \frac{E_a(T_a - T_u)}{R\, T_a^2\, Le_r}(\Phi - 1)$$

<div align="right">(A.21)</div>

where n and m are the orders of the lean and rich reactant, T_a and T_u are the adiabatic and unburned temperatures, and Φ is the equivalence ratio of the mixture.

APPENDIX B - Aluminum Combustion Model Derivation

The derivation of the aluminum combustion model used here will now be described. For comparison of this derivation to that done by Law (1973), see the original work. The mass fluxes of the various species in Region A (between the particle and the flame) and Region B (between the flame and infinity) are based on the mass flux of metal (M_f) away from the surface of the particle (See Table B.1)

Table B.1

Mathematical Descriptions of Species
in the Aluminum Combustion Model

Species	Region A	Region B
Vaporized Metal	M_f	--
Oxidizer Species i	--	$M_{i,B} = \lambda_i\, \nu_i\, M_f$
Vaporized Metal Oxide	$M_{v,A} = -\theta\, \nu_p\, \eta\, M_f$	$M_{v,B} = \theta\, \nu_p\,(1-\eta)\, M_f$
Condensed Metal Oxide	$M_{c,A} = -(1-\theta)\, \nu_p\, \xi_A\, M_f$	$M_{c,B} = (1-\theta)\, \nu_p\, \xi_B\, M_f$

The symbols θ and η represent the fraction of oxide product that is vaporized and the fraction of vaporized product which moves toward the particle surface, respectively. The symbol ν is the stoichiometric mass ratio of oxide or oxidizer to metal. The symbol λ is the fraction of metal which reacts with the particular oxidizing species. ξ_A and ξ_B are the fraction of condensed products which move inward or outward respectively. By separately summing the terms involved with inward flow and outward flow, the total flow in these regions can be determined.

Species Equation Solution

The equation for conservation of species (Bird, et. al., 1960) can be written as:

$$\frac{\partial}{\partial t}\rho_i = -(\nabla \cdot \{\rho_i \vec{V} + \vec{j}_i\}) + r_i$$

<div align="right">(B.1)</div>

Since the model is considered to be quasi-steady state. similar to the original model of Law, the time dependency can be removed. In addition, the reaction is considered to be a boundary condition only at the flame, thus the reaction term can also be removed. Assuming Fick's law of diffusion and spherical symmetry. the following result is obtained.

$$\frac{1}{r^2}\frac{\partial}{\partial r}\left\{r^2\left(\rho v Y_i - \rho_g D_{ij}\frac{\partial Y_{i,g}}{\partial r}\right)\right\} = 0$$

(B.2)

In this equation, Y_i, ρ, $Y_{i,g}$, and ρ_g are the overall and gaseous mass fraction and density and D_{ij} is the diffusivity of component i in the gas mixture. It can be shown that

$$Y_i = (1 - Y_c)\,Y_{ig}$$

(B.3)

$$\rho_g = \rho\,\frac{(1 - Y_c)}{(1 - R)}$$

(B.4)

where Y_c is the mass fraction of condensed phase and R is the volume fraction of condensate. By substituting these expressions into Equation (B.2), assuming R is small, and integrating, the result is the mass flux of a given species.

$$m_i = 4\pi r^2 \rho\left\{v Y_i - D_{ij}\frac{\partial Y_i}{\partial r}\right\}$$

(B.5)

The radial distance can then be non-dimensionalized with respect to the particle radius (r_s), and the mass flux (m) with respect to the term $4\pi\rho D r_s$. The resulting expression is then integrated from the flame to any radial location to obtain the expression:

$$M\left(\hat{r}^{-1} - \hat{r}_f^{-1}\right) = \ln\left\{\frac{MY_{i,f} - M_i}{MY_i - M_i}\right\}$$

(B.6)

where the non-dimensional term M is the total mass flux, M_i is the mass flux of species i, $\hat{r}_f$ is the non-dimensionalized flame radius, and $Y_{i,f}$ is the mass fraction at the flame.

Energy Equation Solution

The energy equation can be solved similarly to the species equation using the equation (Bird, et. al., 1960):

$$\frac{\partial}{\partial t}\rho H = -\left(\nabla\cdot\rho\vec{v}H\right) - \left(\nabla\cdot\vec{q}\right) - \left(\tau:\nabla\vec{v}\right) + \frac{Dp}{Dt} + Q_r$$

(B.7)

By assuming steady-state and no shear in a region free of sources and sinks. the energy equation in terms of enthalpy can be written as

48

$$-\left(\nabla \cdot \rho \vec{v} H\right) - \left(\nabla \cdot \vec{q}\right) = 0 \qquad (B.8)$$

where H is the specific enthalpy. By assuming Fourier's law of heat conduction, spherical symmetry, and performing one integration, one can obtain the expression:

$$\rho v H - 4\pi r^2 k \frac{\partial T}{\partial r} = constant \qquad (B.9)$$

The total mass flux times the enthalpy can then be written as the sum of the individual components resulting in the equation

$$\sum h_i m_i - 4\pi r^2 k \frac{\partial T}{\partial r} = constant \qquad (B.10)$$

By following a similar non-dimensionalization for radius and mass flux and non-dimensionalizing temperature in terms of the ratio of heat capacity and heat of vaporization,

$$\hat{T} = \frac{C_p T}{\Delta H_{vap}} \qquad (B.11)$$

the following expression is obtained.

$$\sum h_i M_i - Le\, \hat{r}^2 \frac{\partial \hat{T}}{\partial \hat{r}} = H \qquad (B.12)$$

In this equation, H is the total amount of energy flux in either the inner or outer region. The reaction is divided into two parts: the reaction of the aluminum to a vaporized metal oxide and the condensation of the vaporized metal oxide. The reference temperature of species enthalpy is the droplet surface temperature. The non-dimensionalization of enthalpy and heat of reaction is done with respect to the heat of vaporization. The enthalpies of the various components are shown below:

Aluminum	$\hat{h}_f = \hat{T} - \hat{T}_s$
Oxidizer Species	$\hat{h}_o = \hat{T} - \hat{T}_s$
Vaporized Oxide	$\hat{h}_v = -\hat{Q}_1 + \left(\hat{T} - \hat{T}_s\right)$
Condensed Oxide	$\hat{h}_c = -\hat{Q} + \left(\hat{T} - \hat{T}_s\right)$

$$(B.13\text{-}16)$$

where the total heat of reaction of the aluminum Q is equal to the sum of the two components Q_1 (vaporized oxide) and Q_2 (condensation of oxide). By assuming infinitely fast vaporization and condensation, the flux of heat at the particle surface can be determined by the heat of vaporization of the aluminum, heat of condensation of the oxide vapor and the radiative heat flux between the particle and the flame:

$$\left\{ k\frac{\partial T}{\partial r}\right\}_s = M_f\Delta H_{vap} + M_{v,A}Q_2 - Q_{r,A} \tag{B.17}$$

Substituting the nondimensionalized form of equation B.17 into equation B.12 for the particle surface, an expression for the energy flux in the inner region results. When condensed oxides are trapped at the flame, the heat associated with them is not transported energy, but is rather is lost. In addition, heat loss occurs due to radiation from the flame. The energy fluxes in Region A and B in non-dimensional form can be written as

$$H_A = M_{v,A}Q - M_f + M_{c,A}Q\xi_A + Q_{r,A} \tag{B.18}$$

$$H_B = H_A - M_{c,f}h_{c,f}(1-\xi_A-\xi_B) - Q_{r,B} \tag{B.19}$$

where $Q_{r,1}$ and $Q_{r,2}$ are the radiative heat flux at the surface and flame, respectively. With these quantities known, equation B.12 can now be integrated from the flame to some radial distance r. The resulting equation is found to be

$$M(\hat{r}^{-1} - \hat{r}_f^{-1}) = - Le \ln\left\{ 1 - \frac{F(\hat{T}_f - \hat{T})}{F(\hat{T}_f - \hat{T}_s) - \varphi}\right\} \tag{B.20}$$

where φ is given by $\varphi = (M_v\hat{Q}_1 + M_c\hat{Q} + H)M_f^{-1}$ and F is the ratio of total mass flux to fuel mass flux.

By applying the boundary conditions at the particle surface, flame, and at infinity, a set of equations describing the species concentration and temperature in the inner and outer region result as seen in Table B.2.

These equations are then combined to form i+1 independent equations and i+2 unknowns (where i is the number of oxidizing species). To complete the degrees of freedom, we recognize that the sum of the fraction of oxidizer must be equal to one. The i+2 equations are solved using a multivariate Newton-Raphson technique. Relaxation must be included for the equations to reach convergence.

Table B.2

Species Concentration and Temperature Equations
In Regions A and B

Region A

Aluminum

$$M_f F_A\left(1 - \frac{1}{\hat{r}_f}\right) = -\ln\left[1 - F_A Y_{f,s}\right]$$

Vaporized Oxide

$$M_f F_A\left(1 - \frac{1}{\hat{r}_f}\right) = \ln\left[1 + \frac{F_A Y_{v,f}}{\theta v_p \eta}\right]$$

Temperature

$$M_f F_A\left(1 - \frac{1}{\hat{r}_f}\right) = Le_A \ln\left[1 + \frac{F_A(\hat{T}_f - \hat{T}_s)}{1 - \hat{Q}_2 \theta v_p \eta - \hat{Q}_{r,A}}\right]$$

Region B

Oxidizer

$$M_f F_B\left(\frac{1}{\hat{r}_{inf}} - \frac{1}{\hat{r}_f}\right) = -\ln\left[1 + \frac{F_B Y_{i,\infty} D_i}{\lambda_i v_i D_B}\right]$$

Vaporized Oxide

$$M_f F_B\left(\frac{1}{\hat{r}_{inf}} - \frac{1}{\hat{r}_f}\right) = \ln\left[1 - \frac{F_B Y_{v,f}}{\theta v_p(1 - \eta)}\right]$$

Temperature

$$M_f F_B\left(\frac{1}{\hat{r}_{inf}} - \frac{1}{\hat{r}_f}\right) = -Le_B \ln\left[1 - \frac{F_B(\hat{T}_f - \hat{T}_\infty)}{F_B(\hat{T}_f - \hat{T}_s) - \phi_2}\right]$$

51